Politecnico di Milano
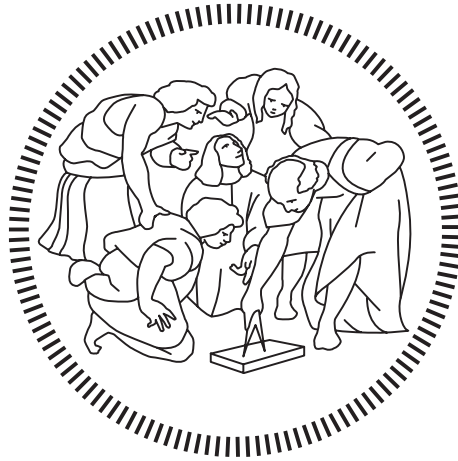
SCHOOL OF INDUSTRIAL AND INFORMATION ENGINEERING

Master of Science – Energy Engineering

Model-based investigation of an industrial microgrid with highly variable loads

Supervisor
Prof. **Emanuela COLOMBO**

Co-Supervisors
Ing. **Giacomo MANZONI**
Ing. **Lorenzo RINALDI**

Candidate
Amin FARZANEHNIA – 926945

Academic Year 2020 – 2021

Acknowledgements

Especially to all those who seek to improve the lives of others by becoming better human beings themselves and who have the insight to find a balance between advancement and maintaining the habitability of our lonely planet for future generations.

Sommario

Una microgrid è un sistema di alimentazione su piccola scala che comprende la generazione di energia distribuita, lo stoccaggio di energia e il carico. In questa tesi, vengono analizzate la promozione e l'ottimizzazione di una microgrid per applicazione industriale. Nel contesto del piano di sviluppo del paese, che si propone di di raggiungere una quota del 100% di energie rinnovabili entro il 2035, ridurre la dipendenza dall'inaffidabilità della rete elettrica di utilità e minimizzare il costo dell'elettricità generata dal diesel utilizzando la tecnologia fotovoltaica, la microgrid contribuisce ad aumentare la quota di energie rinnovabili in Gibuti. Il sistema di interesse è una microgrid con un carico altamente variabile. L'indagine del carico suggerisce soluzioni come soft starter e azionamenti a frequenza variabile, che portano al risparmio energetico. Inoltre, viene considerata la fattibilità economica delle soluzioni. Il mix energetico e la dimensione della microgrid sono ottimizzati utilizzando il codice open-source MicroGridsPy basato sulla programmazione lineare mixed-integer. Pertanto, una microgrid ibrida è ottimizzata come soluzione economica per il carico industriale esistente. Diversi scenari sono studiati per analizzare la fattibilità del sistema studiato. Inoltre, l'ottimizzazione stocastica con diversi scenari di carico viene eseguita per valutare meglio la condizione attuale del carico e tenere conto del probabile aumento futuro della domanda di carico. Si dimostra che utilizzando la gestione del carico dal lato della domanda, si ottiene una riduzione del costo attuale netto, miglioramenti di altri parametri economici e riduzioni di energia a causa della natura intermittente delle energie rinnovabili. Infine, viene eseguita un'analisi di sensibilità per valutare la robustezza del metodo utilizzato.

Parole chiave: Off-grid; Microgrid industriale; Sviluppo di Gibuti; Energia solare; Curva di domanda di carico; Costi delle tecnologie; Analisi economica; Ottimizzazione.

Abstract

A microgrid is a trending small-scale power system comprising distributed power generation, power storage, and load. The promotion and optimisation of an industrial microgrid in Djibouti are studied in this thesis. The microgrid helps reduce the dependency on unreliable utility grid electricity and minimize the cost of electricity generated by diesel. Furthermore, governments incentives encourage industries to promote renewable energies and sustainability. Djibouti development plan, for example, is to achieve a 100% renewable share by 2035. A case study has been presented for an industrial plant with variable loads. The investigation of the load suggests solutions such as soft starters and variable frequency drives, which lead to energy savings. The economic feasibility of the solutions is also considered. The microgrid energy mix and size are optimised using the open-source code MicroGridsPy based on mixed-integer linear programming. Therefore, a hybrid microgrid is optimised as a cost-effective solution for the existing industrial load. Several scenarios are investigated to analyse the feasibility of the studied system. Moreover, stochastic optimisation with different load scenarios is performed to assess better the actual condition of the load and account for probable future load demand increase. It is shown that demand-side load management is necessary due to the intermittent nature of renewable energies leading to reduced net present cost and improvement in other economic parameters. Finally, a sensitivity analysis is performed to evaluate the robustness of the method utilized.

Keywords: Off-grid; Industrial microgrid; Djibouti development; Solar energy; Load demand curve; Costs of technologies; Economic analysis; Optimisation.

Table of Contents

List of Figures

List of Tables

Chapter 1
Introduction

The term "power grid" has traditionally been referred to as the electrical system's four main operating functions: generation, transmission, distribution, and control. The conventional power system relied on centralized generation from high-capacity conventional generators located distant from end-users. In contrast, microgrids are trending power systems consisting of power generation, power storage, and load [1]. According to Electropedia [2], a microgrid is a collection of interconnected loads and distributed energy resources with well-defined electrical boundaries that create a local electric power system at distribution voltage levels, which could operate in grid-connected and island mode.

1.1   Microgrids

Microgrids play an essential part in the transition from a centralized to a distributed decentralized electricity system. They are built with the capacity to isolate themselves from bigger grids, making them operationally resilient. They have the ability to function in grid-connected as well as islanded (i.e. stand-alone) modes. The microgrid is in islanded mode when it operates and controls its own power generation, manages and serves system load demand, and regulates system stability. The advantages of microgrids are as follows:

- High efficiency and reduced cost electricity
- Highly dynamic response for an energy source
- Encouraging local empowerment by economic growth and job provision
- Integration of various power sources
- Reduce transmission losses
- Increase power reliability
- Solves the grid congestion issue
- Strengthening the utility grid

On the other hand, microgrids have several challenges in their development, such as control, protection, energy management, and economic planning.

Other challenges in the implementation of microgrids are related to policy, technology, and business. Technical challenges while installing microgrids are as follows:

Today's transmission lines (feeders) are usually used for high capacity power generation. There are challenges with feeder availability for the microgrids [3].

Secondly, the various scenarios of microgrid generation and demand should be identified and planned for temporary switchover and emergency shedding [1].

Tripping of power sources or short-circuit fault occurrences are unusual disturbance issues in the microgrids. Microgrids are made up of various power sources and equipment. Maintaining system stability with inertia-based generators, as well as static converter-based PV, wind, and energy storage devices is a difficulty. Furthermore, there are several types of converters, including those based on power-electronic devices and virtual synchronous generators. To preserve system stability, manufacturers and designers should perform a comprehensive study of equipment.

To get the most out of a microgrid, it is critical to have a good design and functional analysis of the control system. The mode of operation and settings of the microgrid are essential while designing the microgrid control system. To successfully handle the operating scenario, the control system must integrate each promising control technique [4,5].

Finally, a complete testing and validation specification must be defined to verify that, in the event of a real-world scenario, the microgrid controller makes the most likely and approved option based on the set criteria and constraints. Furthermore, before conducting the operation, compatibility with the layers of the microgrid system should be described and tested.

Microgrids are generally categorized into grid-connected (i.e., on-grid) and isolated (off-grid) [6] according to the connection to the utility grid (Figure 1.1) [7]. In a grid-connected microgrid, when the national grid is operational, it helps meet the remaining energy demand that PV panels and batteries cannot provide. Moreover, PV, battery, and a diesel generator are the only energy sources available when there is a power outage. PV plays a critical function, and when the demand is higher, the battery energy storage system is utilized. The generator is used to supply any remaining unmet load and, if required, charge the batteries [8].
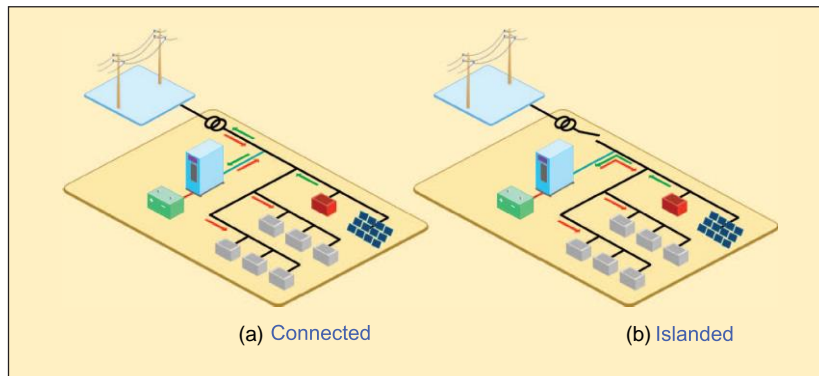
Figure 1.1 Microgrids modes: a) grid-connected and b) off-grid [7]

Based on location, microgrids are classified into two broad categories of urban and remote microgrids. Urban microgrids are built in the vicinity of towns and cities. They have the capability of operating in both grid-connected and stand-alone modes. They are installed in commercial and housing premises, including hospitals, universities, industries, etc. Remote microgrids, on the other hand, exist in areas where utility power is not present due to geographical situations or lack of development. Hilltop, island, and rural areas are examples of remote microgrids. They are operating in stand-alone mode [1].

1.1.1   Industrial Microgrids

The industrial sector accounted for 29 % of the total final electricity consumption in the year 2019 [9]. The interest in using distributed generation is increasing rapidly due to distribution and transmission losses regarding central power plants and due to the pressure to increase renewable electricity production. Commercial and industrial microgrids account for 24.1% of the total microgrid installed capacity [3]. The operation objective of an industrial microgrid is to increase energy efficiency, control emissions, use renewable energies, and expand security and reliability [10], and minimize operation and maintenance costs [11].

1.2   Literature review

Hanrahan et al. [12] studied a visualization tool for electricity flow at industrial sites with combined heat and power (CHP) and wind generation. Larger renewable capacities benefit from economies of scale but limiting the quantity of power exported from the site is also necessary to avoid paying higher network infrastructure usage fees. As a result, the best scenario is to increase the amount of site load provided by on-site generating. They investigated a test case consisting of wind power with a CHP system with control of on-site generation. The control maximizes the share of wind energy utilized on-site. They showed that the type of energy sources, the size of each generator, current and future load are of most

important driving factors for the industrial sites. Moreover, the control system for dispatchable electricity should be considered in the analysis.

Guarnieri et al. [7] reviewed the design of a multi-technology microgrid in Venice, Italy. The microgrid has a 400 V DC bus which works in both on-grid and off-grid modes. It uses a biodiesel generator and photovoltaic system in addition to lithium (Li), lead (Pb), sodium (Na), vanadium, and hydrogen energy storage systems. The microgrid is controlled by an energy management system with a supervisory-control-and-data-acquisition-like architecture, which includes features like anti-islanding, low-voltage ride through, and black start. Traditionally, a mismatch between the load and supply of energy in a power system was addressed by a fast increase in supply, which was typically costly and resulted in high emissions. However, with a microgrid system, it is preferable to make operational changes on the demand side, such as demand-side management (DSM) and demand response (DR) approaches.

Recent microgrids are built with a high renewable energy fraction. Renewable energies, however, are intermittent in nature. So, the peak load could occur when the energy production is low. This imbalance could be solved by energy storage and diesel generator backup. Moreover, load-side management is another method to increase system functionality. Controllable loads have the possibility to be reduced in critical times and scheduled when the generation is maximum. Controllable loads respond to a control signal by attaining a step-change in power consumption, which might be based on a price signal or a power supply disruption [13].

Logenthiran et al. [14] performed demand-side management in smart grid using Heuristic optimisation tool in residential, commercial, and industrial facilities. Demand-side management allows consumers and customers to make the decision of energy-saving and lead to reduced peak demand. The results of demand management are reduced CO_2 emission and reduced overall operation and maintenance costs. The day-ahead load shifting approach described in this work is a mathematical formulation of a minimization problem using an Evolutionary Algorithm. Their results demonstrate that the suggested algorithm can manage a large number of controlled devices and lead to economic saving while lowering the smart grid's peak power demand.

Traditionally, a mismatch between the load and supply of energy in a power system was addressed by a rapid increase in supply, which was typically costly and resulted in high emissions. However, it is preferable to make operational changes on the demand side with a microgrid system, such as demand-side management (DSM) and demand response (DR) approaches.

Logenthiran et al. [15] performed DSM in smart grid using Heuristic optimisation tool in residential, commercial, and industrial facilities. DSM allows consumers and customers to make the decision of energy-saving and lead to reduced peak demand. The results of demand management are reduced CO_2 emission and reduced overall operation and maintenance costs. The day-ahead load shifting approach described in this work is a mathematical formulation of a minimization problem using an Evolutionary Algorithm. Their results demonstrate that the suggested algorithm can manage a large number of controlled devices and lead to economic saving while lowering the smart grid's peak power demand.

Blake and O'Sullivan optimised distributed energy resources in an existing industrial microgrid in Ireland. The test facility is connected to the electrical grid, but it also contains onsite generation, including a wind turbine and a combined heat and power (CHP) unit. They showed that the use of microgrids might result in significant cost reductions compared to an industrial plant that is only powered by grid energy. Moreover, when a demand response scheme based on pricing is implemented, further savings are realized since the load is lowered during periods of high electricity rates. A significant decrease in CO_2 emissions may be achieved by utilizing renewables in an industrial microgrid.

A planning approach for the industrial microgrid is provided based on Internet of Things and Knowledge Discovery in Databases techniques to reduce the impact of industrial operations on the environment [16]. If planning engineers are capable of designing a power supply system that is not only focused on historical demand data, but also on manufacturing and environmental data, industrial microgrid development might be a step forward towards more sustainable manufacturing processes. The goal is to create a microgrid that enables the identification, planning, and implementation of energy-saving methods at the supply, management, and consumption levels. The full potential of energy savings for a microgrid can be determined through a holistic analysis of the plant's entire value chain: not only from the standpoint of generation and distribution but also from the standpoint of consumption and manufacturing process requirements. These techniques could be utilized to reveal hidden cost-cutting opportunities, assisting in the successful implementation of improved business choices.

Lu et al. [17] presented a deep learning-based energy management scheme for industrial microgrids. An adaptable online energy management scheme for industrial microgrids is presented that minimizes electricity costs while meeting production demand using an optimisation problem repeatedly solved over a moving control window, considering forecasted future prices and renewable energy profiles. The optimization is implemented by a hybrid deep learning model to forecast future renewable profiles and power costs in a dynamic manner. Their results show the usefulness of the proposed online scheme compared with a microgrid with fixed static prices.

Industrial prosumers in industrial microgrids use self-owned distributed energy resources (e.g., energy storage, combined heat and power (CHP), wind generation, and photovoltaic systems) and buy electricity and natural gas from utilities to meet their multi-energy needs. On the other hand, they sell the excess electricity to the grid or the local community. Electricity, natural gas, heating, cooling, compressed air energy, etc., are time-varying energy requirements of an industrial microgrid. Because the costs fluctuate over time in the electricity market, a sound energy management plan that includes energy consumption optimisation in response to changing energy prices can result in cost savings for industrial applications [18].

A strategy for isolated industrial microgrid energy management is proposed by Eseye et al. [19] using a Modified Particle Swarm optimisation. They studied the development and analysis of a 24-hour ahead optimum energy management system. The microgrid includes wind, PV solar, diesel engine, microturbine, and energy storage. The fundamental purpose of the microgrid EMS optimisation model is to reduce energy production costs as much as feasible, maximize the economic value of energy storage, and optimise renewable energy consumption. Their model accounts for variations in renewable energy supplies and load demands inside the microgrid and use suitable forecasting to mitigate these variations. Furthermore, they tested and validated the results on a real microgrid in China. The simulation outcomes suggest that the proposed method is robust, resulting in a lower overall energy production cost. Furthermore, the suggested technique is rapid convergent and produces global optimum solutions that can be used to manage real-time energy in microgrids with any number of distributed generations and configurations.

Zhang et al. [18] proposed a regret-based stochastic energy management production scheduling for an industrial microgrid. In the energy management of a microgrid for battery manufacturing, they used production task scheduling with production constraints. They defined the model as a mixed-integer linear programming (MILP) problem based on stochastic programming, with day-ahead electricity market pricing and PV power output uncertainty taken into account. They showed that using the technique may successfully plan production tasks in response to market price signals, lowering the cost of energy procurement.

Naderi et al. [20] investigated the optimal planning for a developing industrial microgrid with sensitive loads. The studied system is planned to be implemented in a real industrial site consisting of Computer Numerical Control (CNC) machines. In order to operate for lengthy periods of time, these pieces of equipment require consistent and reliable electricity. They considered three objectives in microgrid planning: ensuring the long-term and secure operation of CNC machines as sensitive loads, minimizing microgrid construction and operation costs, and utilizing available capacities to maximize the renewable energy share,

resulting in a reduction in air pollutants, particularly carbon dioxide (CO_2). They studied different results using HOMER software and found the optimal solution for the industrial site.

Choobineh and Mohagheghi [11] performed a multi-objective energy and asset management optimization in a grid-connected industrial microgrid regarding a vehicle cockpit assembly plant. They considered asset management, emission control, and utilization of alternative energy resources in addition to cost reduction as objective functions. The optimisation problem was a nonlinear mixed-integer type. They studied and optimised the system using different frameworks.

1.3   Motivation and background

The traditional power system is based on the generation of energy from fossil fuels. At the same time, the concerns such as increased environmental damages and disadvantaged economic parameters about these systems are increasing. In order to increase the share of renewables in a microgrid in an industrial site in Djibouti, Gommyr Power Networks ltd., company decided to plan and develop a photovoltaic hybrid plant. Other factors for the action are fostering renewable energies as the country's development plan to achieve a 100% renewable share in 2035, the unreliability of the utility grid electricity in Djibouti, also the increased cost of diesel in comparison with PV module costs. The site consists of rock crushers for construction applications.

1.3.2   Load analysis

The system of interest is supplied by a three-phase line voltage of 400 V.

The system loads are a motor with a nominal power of 300 kVA and other necessary loads on the site, such as lighting and small electrical devices.

The load for a week of the crusher site is obtained and recorded using Fluke 87V Industrial Multimeter and at the supply feeder of the site for a week. The load is shown in Figure 1.2. As can be seen in the figure, the load fluctuates significantly during the weekdays. The minimum and maximum energy consumption of 208 kWh and 1,419 kWh occur on Thursday and Sunday, respectively. It is worth noting that Friday is not a working day in Djibouti, and the load is zero.
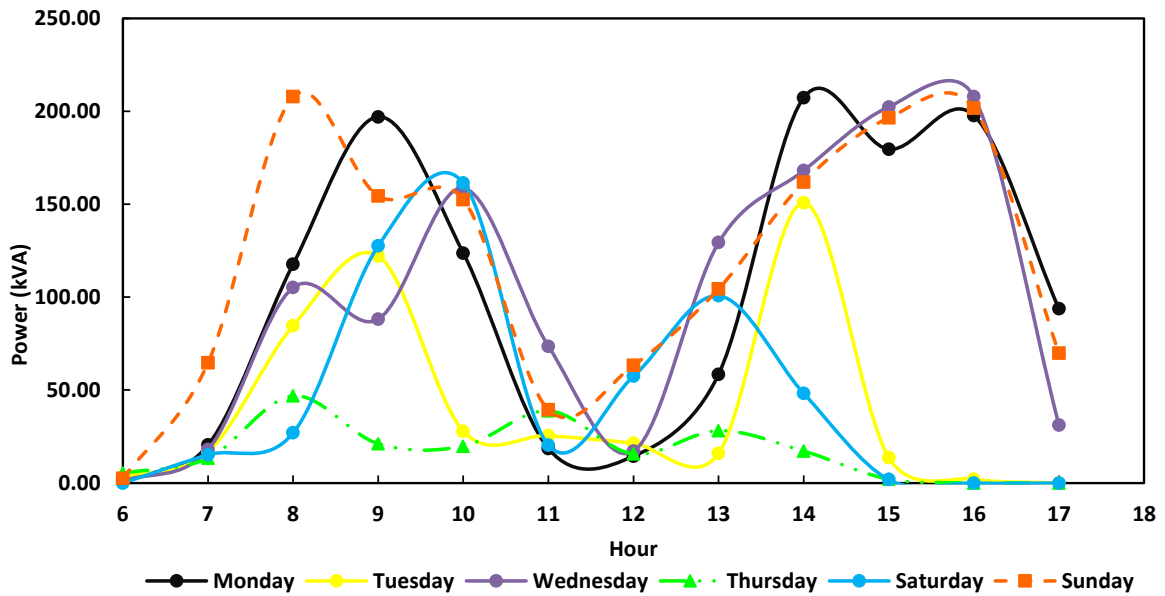
Figure 1.2 The weekly load of the industrial site.

The median value of the load is 149.3 kVA. However, the peak that occurred in the 1-minute measurement is 369 kVA, and the instantaneous power peak is 602 kVA. Figure 1.3 indicates the apparent instantaneous power in a week. The power levels are coloured based on the values as seen in the figure.
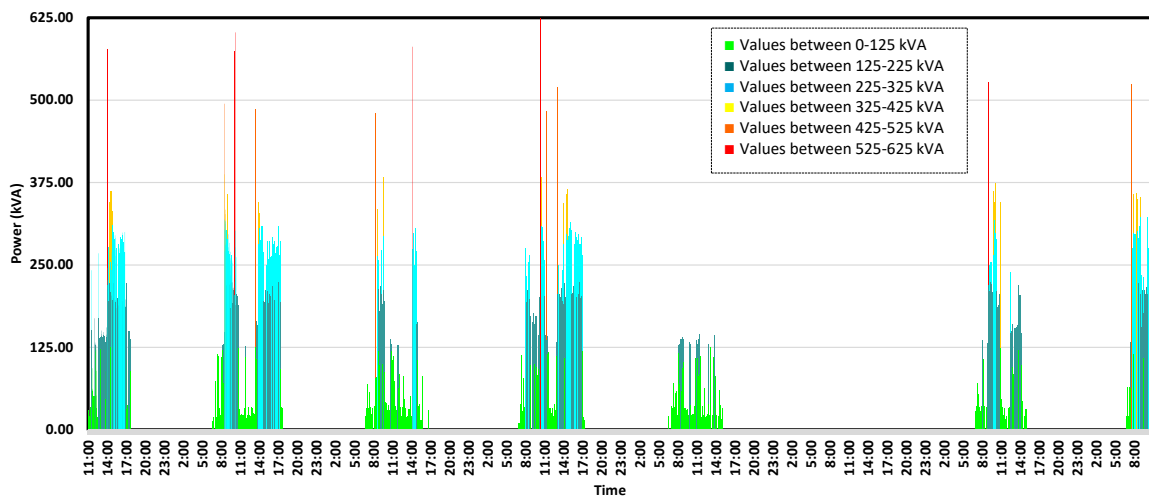
Figure 1.3 The instantaneous power for one week (each colour represents the value range).

Zooming in for Sunday, the power is as shown in Figure 1.4. There are high values of loads occurring two to three times each day.
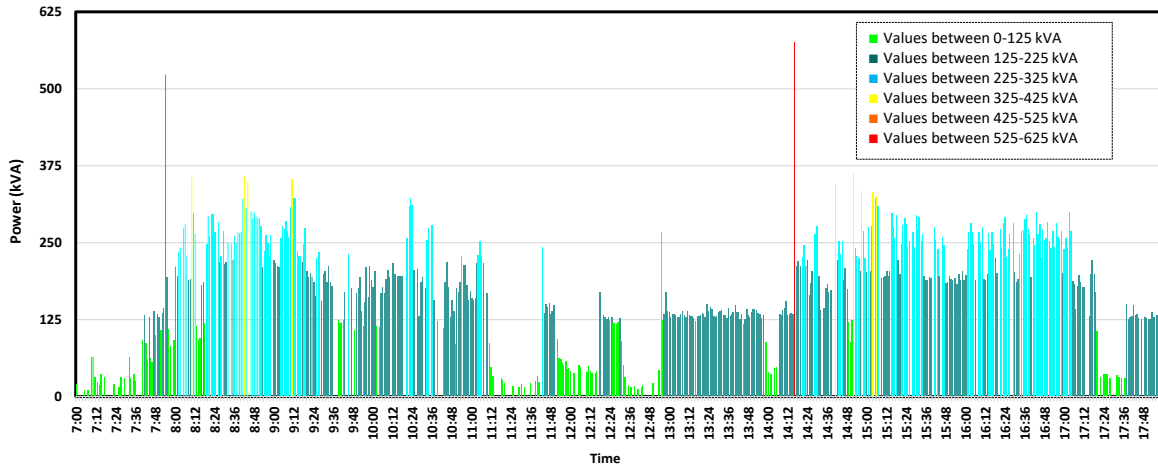
Figure 1.4 The instantaneous power measured on Sunday (each colour represents the value range).

Considering the following assumptions, we have:

- The load is repeating the same every week as measured as the sample week.
- The periods where the load is zero are excluded from the analysis. These periods are occurring beyond the working hours.

The frequency of peak loads is obtained to understand each load level occurrence frequency. The frequency of the load power is in each range of 25 kVA during a week is as shown in Figure 1.5 and Figure 1.6. According to Figure 1.6, the power higher than 325 kVA correspond to less than two per cent of the working condition. Moreover, the median power in working conditions is 149.3 kVA.
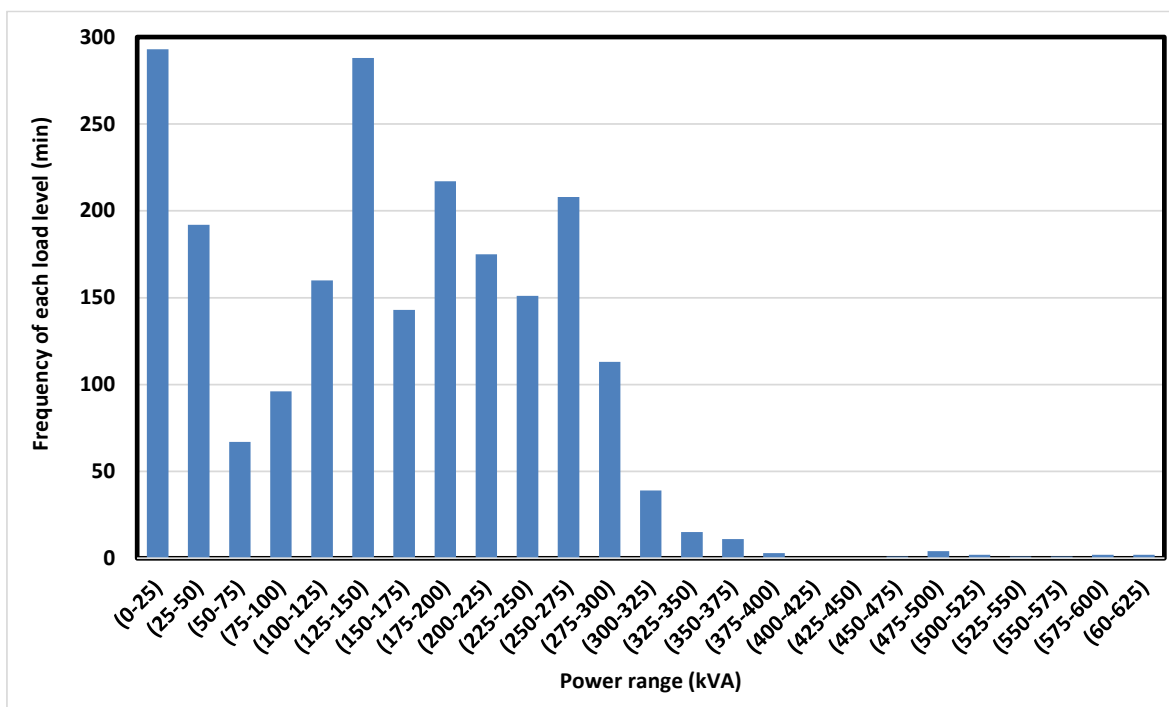
Figure 1.5 Load frequency in a week for each demand level.
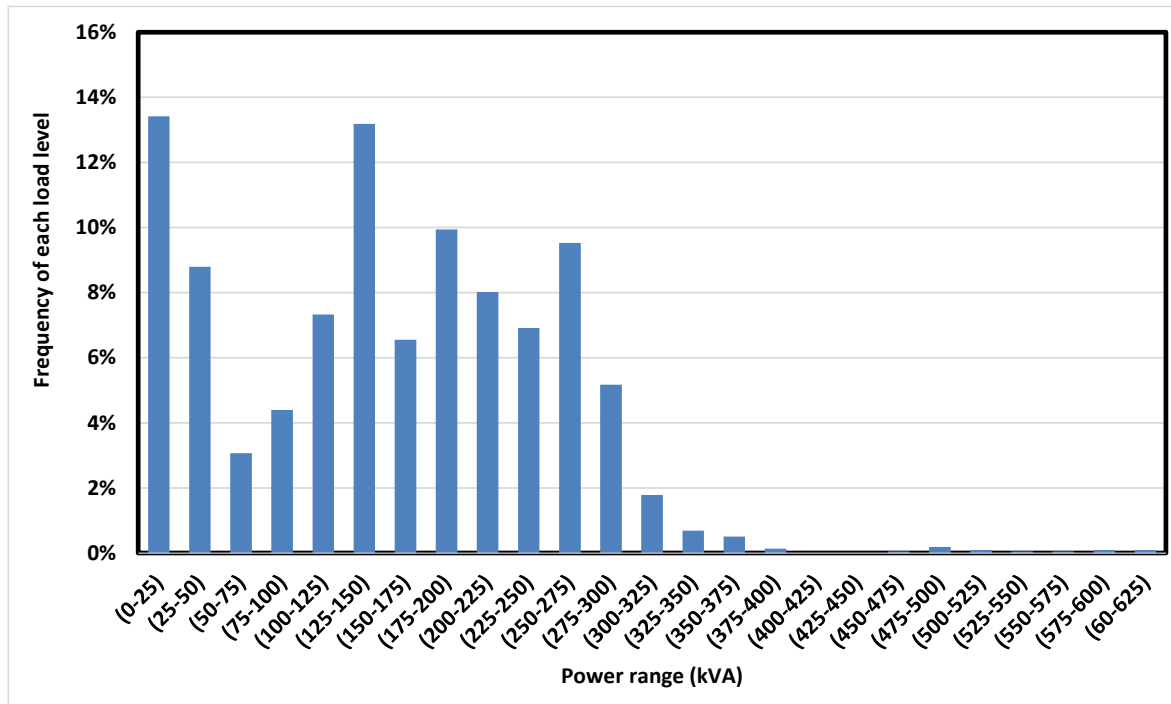
Figure 1.6 Percentage of each load level in the working condition

The load analysis shows that there is a peak in power during 2% of the working condition. These high powers occurring for a short period are due to overcurrent in the system. The maximum instantaneous input current drawn by electrical equipment when initially turned on is known as inrush current, input surge current, or switch-on surge. The inrush current occurs in the startup and shutdown of the electrical equipment.

Since the loads in the Djibouti site consist of mainly electrical motors, the inrush current problem is significant. When motors accelerate to maximum speed, they generally require a substantial quantity of energy. Figure 1.7 show the torque developed by an asynchronous machine while accelerating from zero to maximum speed. On the motor shaft, this is a direct braking force. The motor must be more powerful than the load to accelerate. The difference between the available motor torque and the load torque is the accelerating torque. The starting torque at zero speed is high leading to high values of current and power. The motor must be more powerful than the load to accelerate Soft-starters and variable frequency drives are used to limit the surge power out of the electric motors. Moreover, supercapacitors could be helpful due to their rapid discharge cycle [21].
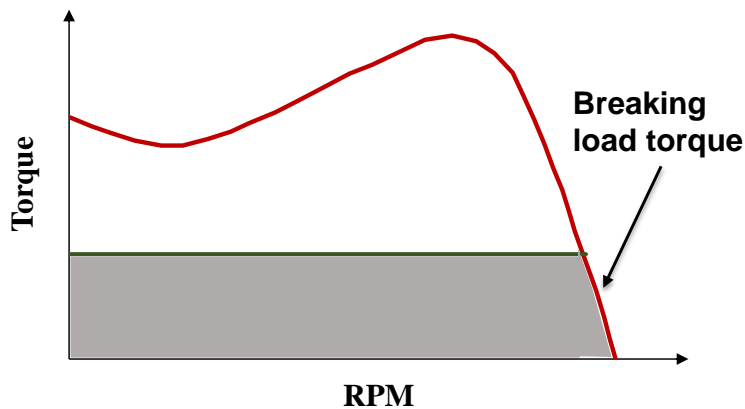
Figure 1.7 The torque developed by a motor while accelerating from zero to maximum speed

1.3.3 Soft-starter

A Soft Starter is a device that allows motors to start with less power than usual. Reducing the power reduces the system's risk of electrical and mechanical shocks [22]. Soft starters consist of controller and overload protection combined in one device. Controllers switch on and off the electric current to the motor. Overload protection prevents a motor from drawing too much current, overheating, and stopping working. The motor overload protection utilized in soft starts is the overload relay. It prevents the motor from overheating by limiting the amount of time the overload current is drawn.

To manage the amount of current given to the motor, a soft starter, also known as a voltage starter, is installed between the motor and the incoming power line. Soft starters allow an AC induction motor to accelerate up more slowly than a typical motor starter, resulting in less current taken. The torque is likewise lower because the voltage becomes lower, resulting in a soft or easy start.

The use cases of the soft-starters are:

- keeping the electricity distribution system from overloading
- Reducing the starting torque to minimize extra wear and tear on equipment.

Moreover, it minimises the voltage drop in the system by reducing the starting torque and mechanical stress. Also, the service and maintenance requirements are reduced.

A soft-starter is comprised of two anti-parallel thyristors per phase, as seen in Figure 1.8.

These thyristors are semiconductor components that are typically isolating but may be made to conduct by providing a firing signal, enabling voltage and current to pass through.

A firing signal is given to the thyristors during a soft start, allowing just the final half-period of each half period of the voltage sinus curve to pass through.

The firing signal is sent earlier and earlier during the start, allowing a larger and larger portion of the voltage to flow through the thyristors.

Finally, the firing signal is transmitted at the zero crossing, allowing 100 per cent of the voltage to flow through.
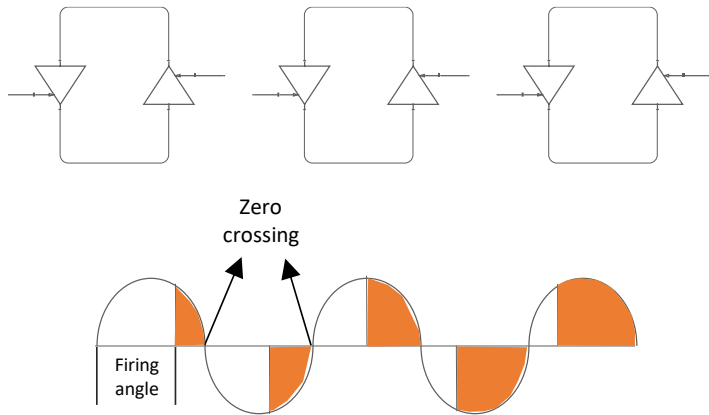
Figure 1.8 Schematic of a soft-starter and the switching of the firing signal while soft starting.

Figure 1.9 show the effect of soft-starter on the motor's starting torque and current. According to the figure, using soft-starter at high load the current and torque increase gradually and the peaks are minimized.

A

B

Low load

High load

C

D

Current

Current without soft-starter

Smooth start

Smooth start
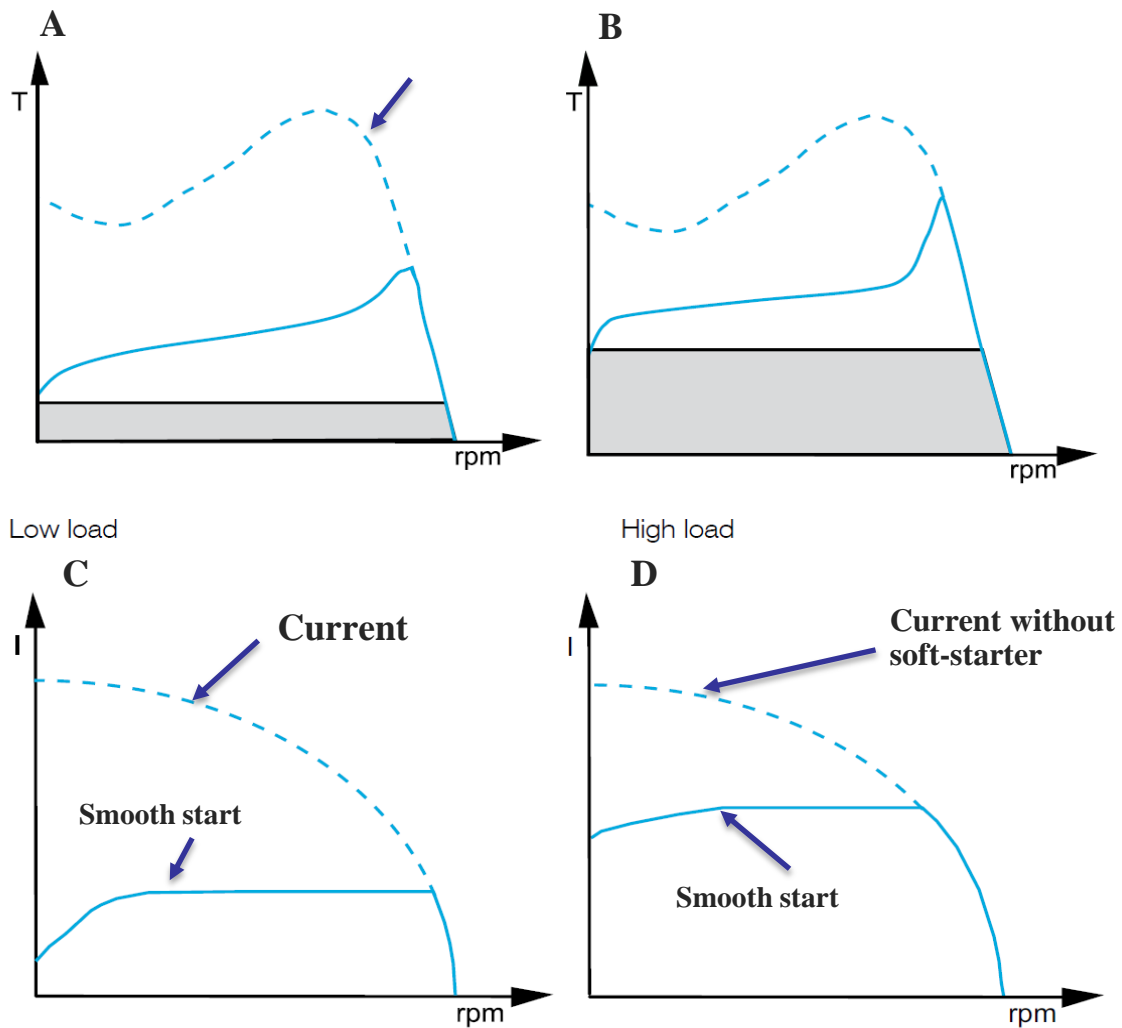
Figure 1.9 The starting torque when using the soft-starter at low and high load (A) and (B), the motor current with soft-starter at low and high load (C) and (D)

Crushers, mixers, mills and stirrers usually have a massive moment of inertia, so the soft-starter is selected larger than the motor kW size. Furthermore, since the big flywheel will cause a long slow down period before the fan stops, a stop ramp should never be used for this kind of application [23].

1.3.4   Variable frequency drives

The other electrical device used for the inrush current is a variable frequency drive. A variable frequency drive (VFD) is a type of motor controller that controls the frequency and voltage of an electric motor's power supply.

The VFD may also control the motor's ramp-up and ramp-down during start and stop, respectively [24]. It consists of two converters. Six diodes make up the first stage of the converter (AC to DC, also called rectifier). Current can only flow in one way through diodes.

As each diode opens and closes, we receive six current "pulses." This is referred to as a "six-pulse VFD," and it is the standard arrangement for Variable Frequency Drives.

Assume that a 480 V system powers the drive. The maximum voltage is 679 volts. The AC ripple on the VFD DC bus is also present. The voltage fluctuates between 580 and 680 volts.

Adding a capacitor to the DC bus helps to eliminate AC ripple. In a plumbing system, a capacitor works similarly to a reservoir or accumulator.

The second converter converts the DC signal to AC with the amplitude and frequency adjusted and changed (often called inverter).

The drive ramps up the frequency from 0 Hz to network frequency during startup (50 or 60 Hz). For that frequency, the motor can be said to be running at its rated speed. As a result, even at startup, the frequency converter functions at minimal current and torque [25].

Using a variable frequency drive has many benefits such as:

- Save energy and boost system performance.
- In hybridization applications, convert power.
- Match the drive's speed to the process's requirements.
- Match a drive's torque or power to the process needs.
- Enhance the working atmosphere.
- Reduced noise levels, such as from fans and pumps
- Machines' lifetimes can be extended by reducing mechanical stress.
- Reduce peak usage to avoid peak-demand pricing and the size of the needed motor.

1.3.5 Cost of drives

Here, a summary of the economy of machine drives is presented. For a system 440 kW, the cost of a variable frequency drive and the soft starter is summarized in Table 1-1.

It should be noted that the cost of the whole system depends on many other factors. These factors include the investment cost, installation cost, and operational cost. The investment cost is essential because using the drives and soft-starters smaller motor size is required. Therefore, using drives the investment cost of motors would reduce. As for installation cost, we might need to install additional devices such as mechanical controllers substitute to modulate the working condition. Finally, considering operational costs, the maintenance, and the energy consumption of motors are reduced significantly using drives [25].

Table 1-1 The cost of drives

Equipment	Cost	Cost per unit
bypass soft starter 440 kW Delixi (Hangzhou) Inverter Co., Ltd. [26]	1,050 $	2.4 $/kW
VFD 440 kW Schneider Electric	~ 60k$	136 $/kW

The VFDs are used for a system in which speed control is required. In the crusher system, speed control is not a priority. Therefore, considering economic values, the need, and system complexity, the best solution is the soft-starter with bypass switching. While there are several mechanical and electrical side effects of VFD control, they are frequently overlooked because they are more difficult to quantify in terms of dollars and cents than the kWh savings, which may be easily quantifiable. These effects, on the other hand, are real and can frequently save as much as the efficiency gains [24].

The present thesis evolved through the five months of internship at Gommyr PN company. During the period, I worked on the microgrid development plans. An industrial microgrid with variable loads in Djibouti is studied, and the various methods for resolving the peak load power issues are proposed. Moreover, surveying the literature suggests that a comprehensive study and optimisation of an industrial microgrid with variable loads is rare. The aim of this thesis is the provision of an analysis of an industrial microgrid. Load analysis is performed on an existing industrial application. The power problem is investigated thoroughly, and solutions are provided. The feasibility of the solutions is studied economically. The microgrid energy mix is optimised in various scenarios using the open-source code MicroGridsPy. Several updates have been contributed to the software that helps faster and more accurate solutions and better visualization. Chapter 1 discusses the industrial microgrid, Djibouti situation and energy potentials. Furthermore, the load of the microgrid and the model MicroGridPy are shortly described along with electrical components such as drives as a solution for the load problem. Chapter 2 discusses the optimisation model used for the microgrid energy mix. Next, the input data used for the optimisation is discussed in Chapter 3. Finally, in Chapter 4, the results of various investigated scenarios are reported.

1.4 Djibouti Scenario

The Republic of Djibouti is a small developing country in the Horn of Africa bordered by Eritrea, Ethiopia, and Somalia, representing Sub-Saharan Africa's energy crisis. The total area is 23,200 km^2, and the total population is 988,002 in the year [27]. The electrification

rate (i.e., the percentage of the population who have access to electricity) is 42%. The essential data indicators are summarized in Table 1-2. Low electrification rates, the unreliability of the existing centralized electrical network, the high cost of fuel, and the scarcity of fossil fuels all make energy one of the top government concerns. Renewable energy utilization is increasingly being considered in the country's energy policy, as it is by other African nations.

Table 1-2 Djibouti's key indicators [27]

Indicator	Value	Year
Population	988 002	2020
Gross Domestic Product GDP (USD Million)	3 384	2020
Gross National Income GNI (USD Million)	5 610	2019
GDP per capita PPP (USD)	5,768.8	2019
GNI per capita PPP (USD)	5,610	2019
CO_2 emissions (metric tons per capita)	0.511	2018
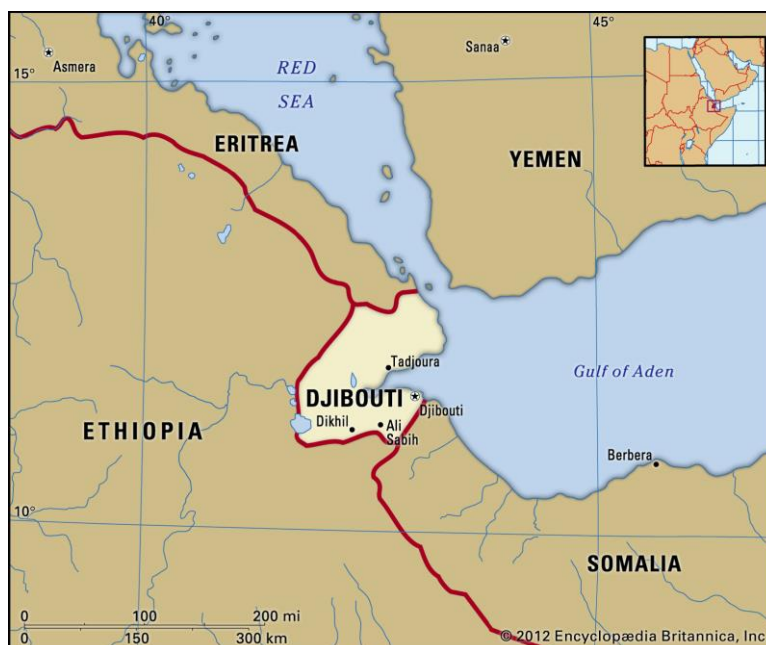
Figure 1.10 Map of Djibouti [28]

1.4.6 Off-grid electricity as a tool for job creation and poverty reduction

Electricity enables individuals in industrialized nations to appreciate lighting, refrigeration, hygiene, and interior climate control in their homes, companies, and schools, as well as extensive access to different electronic and electromagnetic media [29]. Energy enables job creation. Moreover, new jobs will be created as a result of the replacement technologies such as lightning. Through indirect employment, re-spending of energy savings, currency conservation, higher literacy, and improved working conditions, a probable bigger number of extra jobs and employment income will be indirectly generated by developing microgrid technologies. In contrast, research shows that expanding the central grid is unlikely to result in a net gain in employment [30].

On the other hand, the availability and usage of electricity are strongly linked to the quality of life. Figure 1.11 shows the human development index (HDI) versus the annual electricity consumption per capita. It is a United Nations Development Programme (UNDP) index that measures the quality of life and is based on life expectancy, education, and gross national income (GNI) [31]. As seen in the figure, there is a correlation between electricity consumption and the human development index up to a certain point. However, developed nations represent different social and energy patterns, so the electricity uses, and the HDI is not linked.
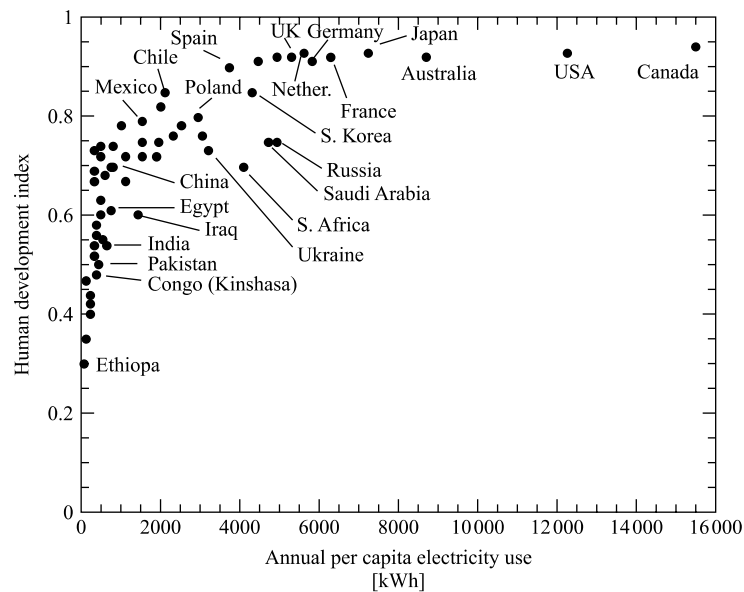
Figure 1.11 Human development index versus the annual electricity consumption per capita [29].

1.4.7 Energy outlook in Djibouti

According to IEA [32], the republic of Djibouti initiated the vision 2035 regarding the long-term development goals and strategies. Education, tourism, fisheries, innovative technology,

industry, etc., are considered in the vision. The vision has set a target to encourage the use of renewable energy resources for power generation. The goal is to actively pursue fossil-to-renewable-energy fuel transition strategies. The following are some of the government's goals:

- Increase the percentage of renewable energy technologies in the energy mix to 87%-100%

- Electricity utility reform

- Renovate and expand the electrical grid.

- Construct new connections.

The target specifies the installation of 200 MW solar capacity (photovoltaic and concentrated solar power), 300 MW wind power, and 500 MW geothermal capacity by 2035.

Imported oil products and traditional biomass fuels are primary sources to meet Djibouti's energy needs. Hydropower supplied from Ethiopia via interconnected grids accounts for about 70% of Djibouti's domestic energy usage. The remaining 30% comes from diesel fuel generating capability that has been installed locally. The utility electricity in Djibouti is expensive, and the country's network infrastructure is prone to outages owing to a lack of maintenance and investment. The country's rising electrical consumption is mainly centred in the capital, while more rural locations have a limited connection to the grid. The amount of installed renewable energies in Djibouti was as low as 0.3 MW (0.21 % of the installed capacity) by the end of 2018. However, a total of 830 MW of renewable energy was under construction in the year 2018. Figure 1.12 depicts energy costs in the industrial sectors, based on estimated average monthly electricity use by various consumers in 20 Arab nations [33]. The average monthly usage for industrial users is 30 MWh. Electricity rates and fossil fuel costs are subsidized in the majority of countries. Nevertheless, they are implementing reforms to modify pricing. In Djibouti, the rate of electricity for the industry is 0.253 $/kWh. It is worth noting that these tariffs are not constant and are linked with the level of consumption.
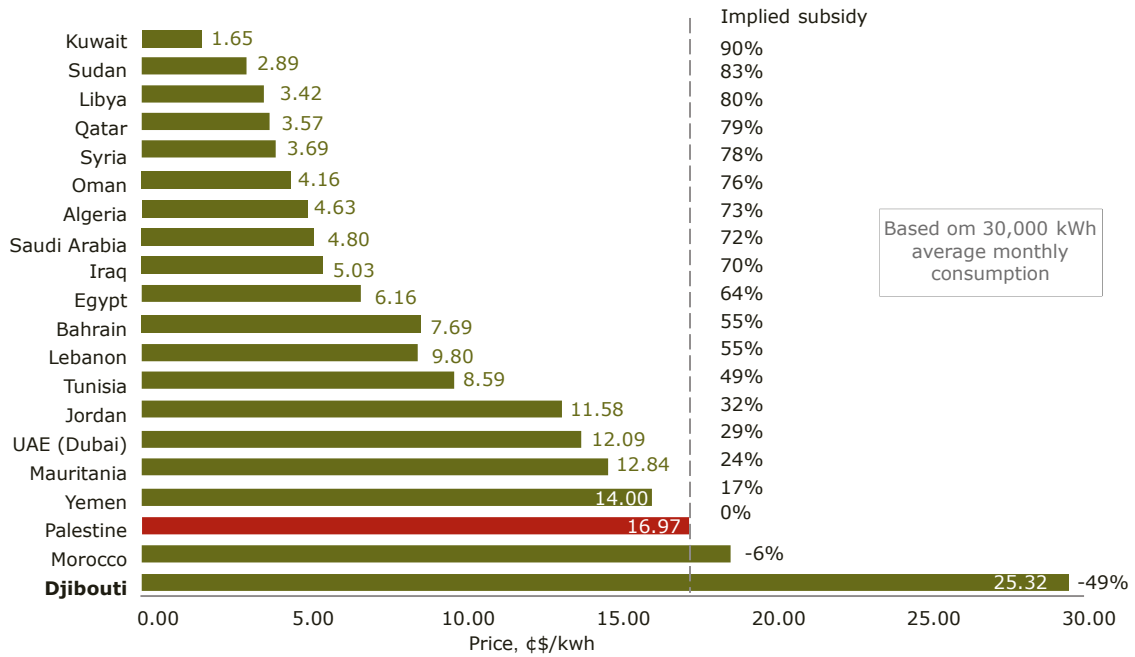
Figure 1.12 Electricity tariff in the industrial sector of the region [33].

Figure 1.13 shows the total renewable energy capacities in the Arab region. The rise in renewable energy capacity in the Arab area is primarily attributable to increases in wind and PV power generation, while hydropower has exhibited a relatively modest growth due to the fact that much of the region's hydro potential has already been exploited [33].
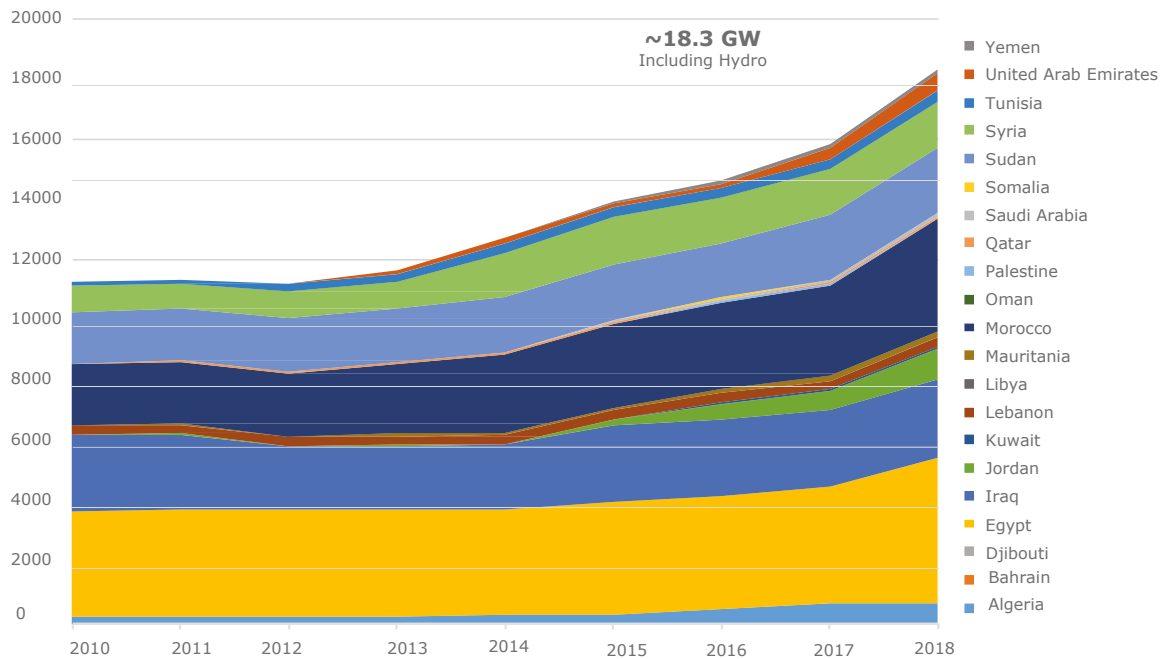
Figure 1.13 Total renewable power installed in the region in the period 2010-2018 [33].

Djibouti has vast solar potential. The Global Horizontal Irradiance (GHI) is 4.5-7.3 kWh per square meter per day (m2/day) across most of the regions, as seen in Figure 1.14 [34].

There are two insolation peak periods (March to April and September to October), with slight daily fluctuation in maximum and minimum radiation levels. From June to August, the hottest and most humid months, the lowest radiation levels are recorded.
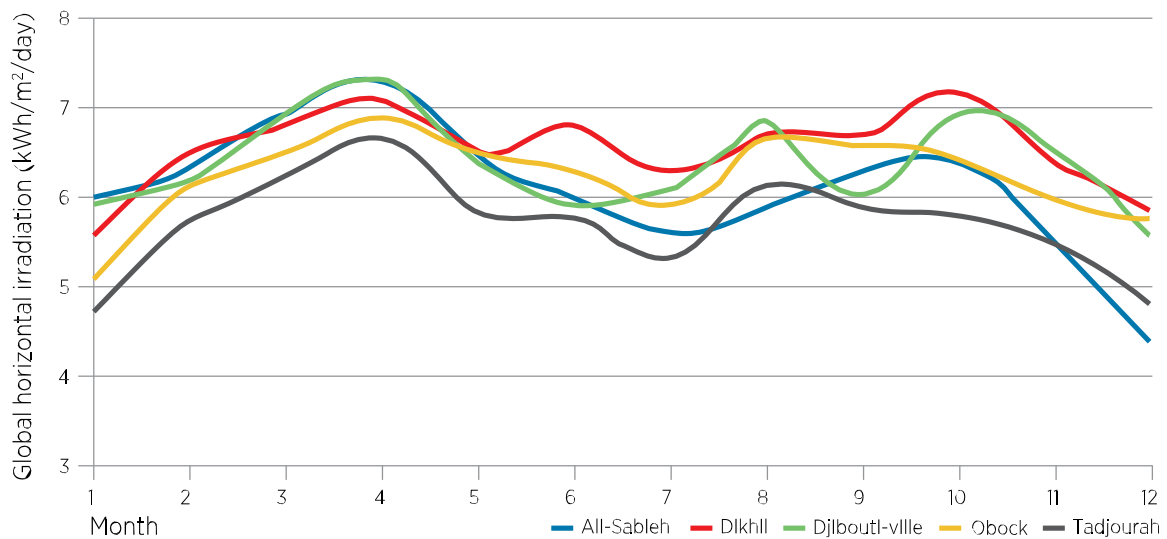
Figure 1.14 Global Horizontal Irradiance (kWh/m2/day) for five sites in Djibouti [34].

Chapter 2
Methodology

2.1   Energy mix optimisation

The MicroGridsPy is an open-source optimisation model that can handle load demand time series that change arbitrarily during the system's lifespan as an input. The model is based on mixed-integer linear programming (MILP) and implemented in the python-based PYOMO language. The code is developed by Balderrama et al. [35]. The optimisation output is the improved system's capacity of each source of energy production also the time series of the least-cost generation or storage technology data throughout the year. Moreover, the fixed and variable costs are obtained for the microgrid [36]. The model has the feature of stochastic optimisation, which helps to minimize the uncertainties [37].

2.1.1   Objective function

The optimisation goal is the estimated net current cost of the project, as expressed in equations (2.1) and (2.2), e is the discount rate, and y is the considered year. inv is the total investment as determined in Equation (2.2), YC is the yearly cost of meeting demand calculated in Equation (2.4), and y is the regarded year, $I_s^{occurence}$ is the specified probability of each scenario. Here, r indicates the renewable source, s refers to the scenario, and t is the time step [38].

$$inv + \sum_{s=1}^{Ss} \left(\sum_{y=1}^{Y} \left(\frac{YC_t}{(1+e)^y} \cdot I_s^{occurence} \right) \right) \tag{2.1}$$

$$\sum_{s=1}^{Ss} I_s^{occurence} = 1 \tag{2.2}$$

The investment cost is calculated by:

$$inv = \sum_{r=1}^{R} U_r^{re} N_r^{re}.C_r^{re} + U^{bat}.C^{bat} + \sum_{g=1}^{RG} U_r^{ge} N_r^{ge}.C_r^{ge} \tag{2.3}$$

where U^{re}, U^{bat}, U^{ge} are the per-unit cost of the renewable source, battery, and the diesel generator, N^{re}, N^{ge} are the number of renewable sources and generators in the microgrid, and C^{re}, C^{batt}, C^{ge} are the nominal capacity of renewable unit, battery and generator unit.

YC the yearly cost of meeting demand is calculated as:

$$YC = Co_s^{OM} + Co_s^{Fuel} + Co_s^{rep} + Co_s^{LL} \tag{2.4}$$

where Co^{OM}, Co^{Fuel}, Co^{rep}, Co^{LL} are the cost of operation and maintenance, cost of fuel, battery replacement, and cost of lost load.

Cost of operation and maintenance is calculated in Equation (2.5), where I_r^{re}, I^{batt}, and I_g^{ge} are the cost of operation and maintenance as a percentage of the total investment incurred each year.

$$Co_s^{OM} = \sum_{r=1}^{R} U_r^{re}.N_r^{re}.C_r^{re}.I_r^{re} + U^{batt}.C^{batt}.I^{batt} + \sum_{g=1}^{G} U_g^{ge}.N_g^{ge}.C_g^{ge}.I_g^{ge} \tag{2.5}$$

The battery longevity has an inverse relationship with the number of cycles it conducts (Cy^{bat}). Equation (2.6) is used to compute this battery replacement cost. The per-unit battery replacement cost (2.6) is denoted by U^{rep}. The unitary cost of the battery's power electronics is U^{elec}.

$$Co_s^{rep} = \sum_{t=1}^{T} E_{s,t}^{bat,ch}.U^{rep} + \sum_{t=1}^{T} E_{s,t}^{bat,dis}.U^{rep} \tag{2.6}$$

$$U^{rep} = \frac{U^{bat} - U^{elec}}{Cy^{bat}.(1 - DOD)} \tag{2.7}$$

Equation (2.8) calculates the lost load cost, where U^{LL} is the per-unit value of the lost load.

$$Co_s^{LL} = \sum_{t=1}^{T} E_{s,t}^{LL}.U^{LL} \tag{2.8}$$

2.1.2 Renewable energy dispatch

The renewable energy dispatch to the microgrid is calculated here:

$$E_{s,r,t}^{re} = \eta_r^{re} . E_{s,r,t}^{re,u} . N_r^{re} \qquad (2.9)$$

where η^{re} is the inverter efficiency corresponding to the renewable source, $E^{re,u}$ is the energy yield per-unit of the renewable source, N^{re} is the number of units installed.

The following limit is also added for the renewable production to be less than the demand $(D_{s,t})$:

$$\sum_{r=1}^{R} E_{s,r,t}^{re} \leq D_{s,t} \qquad (2.10)$$

2.1.3 Battery model

Battery energy storage system is modelled as follows. The energy stored in the battery (EB) is as follows:

$$EB_{s,t} = EB_{s,t-1} + EB_{s,t}^{batt,ch} . \eta^{ch} - EB_{s,t}^{batt,dis} . \eta^{dis} \qquad (2.11)$$

where the energy entering the battery is E^{ch} and energy exiting the battery is E^{dis}, the charging efficiency is η^{ch}, and the discharge efficiency is denoted by η^{dis}.

Constraint for the battery energy storage system are as follows. First the depth of discharge (DOD) should be specified to maximize the lifetime of batteries as defined in equation.

$$C^{bat} . DOD \leq EB_{s,t} \leq C^{bat} \qquad (2.12)$$

The maximum charge and discharge boundaries are specified in equations   and   where $P^{bat,ch}$ and $P^{bat,dis}$ are the charge and discharge limit, $\Delta t^{bat,ch}$ and $\Delta t^{bat,dis}$ are the times required to fully charge or discharge batteries and Δt is the timestep used.

$$P^{bat,ch} = C^{bat} / \Delta t^{bat,ch} \qquad (2.13)$$

$$P^{bat,dis} = C^{bat} / \Delta t^{bat,dis} \qquad (2.14)$$

$$EB_{s,t}^{batt,ch} \leq P^{bat,ch} . \Delta t \qquad (2.15)$$

$$EB_{s,t}^{batt,dis} \leq P^{bat,dis} . \Delta t \qquad (2.16)$$

2.1.4 Diesel generator model

Diesel generators in nominal power operate at the highest efficiency. Partial loading leads to reduced efficiency. However, this is not considered in this case for simplicity and computational limits. The energy output of the diesel is limited by Equation (2.17) [39].

$$E_{s,g,t}^{ge} \leq C_g^{ge}.\Delta t \tag{2.17}$$

where C_g^{ge} is the nominal power of each generator. The cost of energy generation by the generator is:

$$CO_s^{fuel} = \sum_{g=1}^{G} \sum_{t=1}^{T} U_g^{fuel}.E_{s,g,t}^{ge}/(\eta_g^{ge}.LHV_g) \tag{2.18}$$

where U_g^{fuel} is the per-unit cost of the fuel, η_g^{ge} is the efficiency of the generator, and LHV_g is the low heating value of the fuel.

Two constraints are added to the model, which is helpful when the renewable penetration is considered 100% the generator output is zero (Equations (2.19) and (2.20). Moreover, the maximum output of the generator is limited by the load. This constraint would lead to better convergence of the optimised solution and faster computation.

$$\sum_{g=1}^{G} E_{s,g,t}^{ge} \leq D_{s,t} \tag{2.19}$$

$$E_{s,g,t}^{ge} = 0 \; if \tag{2.20}$$

2.1.5 Energy constraint

The energy balance for the microgrid is presented here.

$$D_{s,t} = \sum_{r=1}^{R} E_{s,r,t}^{re} + \sum_{g=1}^{G} E_{s,g,t}^{ge} - E_{s,t}^{bat,ch} + E_{s,t}^{bat,dis} + E_{s,t}^{LL} + E_{s,t}^{curtailment} \tag{2.21}$$

where E^{LL} is the energy that cannot be met by the system.

This energy is constrained by the following:

$$\sum_{s=1}^{S} \left(\frac{\sum_{t=1}^{T} E_{s,t}^{LL}}{\sum_{g=1}^{G} D_{s,t}} \cdot I_s^{occurence} \right) \leq LLP \qquad (2.22)$$

where LLP is the probability of unmet demand. The minimum renewable percentage (renewable penetration) is defined in Equation (2.23).

$$\sum_{s=1}^{S} \left(\sum_{r=1}^{R} \sum_{t=1}^{T} E_{s,r,t}^{re} \cdot I_s^{occurence} \right) \cdot (1 - I^{re}) \qquad (2.23)$$

$$\geq \sum_{s=1}^{S} \left(\sum_{g=1}^{G} \sum_{t=1}^{T} E_{s,g,t}^{ge} \cdot I_s^{occurence} \right) \cdot I^{re}$$

Finally, the number of battery autonomy days is defined as the days the batteries could supply the power:

$$C^{bat} \geq \sum_{s=1}^{S} \left(\frac{\sum_{t=1}^{T} D_{s,t}}{365} \cdot I_s^{occurence} \right) \cdot \frac{N^{bat}}{1 - DOD} \qquad (2.24)$$

Chapter 3
Input data

3.1   Resource assessment

One crucial step to finding the optimal design for a successful microgrid project is to find the energy resources available on the site. The resources available specific to the site of the microgrid should be analysed in the present section. The solar potential of Djibouti makes it a great location for photovoltaic electricity generation in the world, with daily mean irradiation of 5.92 kW/h/m^2 [40]. The Djibouti solar map is shown in Figure 3.1. According to the figure, the yearly sum of solar electricity generated by a module of 1 kWp with an efficiency of 0.75 is between 1650 kWh and 1950 kWh in Djibouti [40].

Because field measurements of solar potentials in remote regions throughout the world are rarely accessible, the site-specific photovoltaic generation throughout the year is created using the software METEONORM v trial 8.0.3. According to the literature, the software is one of the most precise sources for the global radiation data for solar system planning [41,42].

The METEONORM database, version 8.0, contains meteorological data from 1996 to 2015. These data are gathered from many solarimetric stations over a wide range of regions. Although data obtained from solarimetric stations is the most precise, there are times when this source is unavailable near the project site. In these circumstances, the database obtains irradiation data by interpolating satellite data. These interpolations include drawbacks such as uncertainty insertion, inability to collect some meteorological information, difficulties recognizing many layers of clouds, and lack of accuracy in snowy locations [42].

The majority of data sources only offer irradiation measurements in the horizontal plane. To determine a more accurate amount for the energy generated, this data must be transferred to a slanted plane. Perez's approach is found to be more precise in obtaining irradiation data on the slanted plane [43,44]. The software METEONORM has this capability built-in to provide irradiation on a tilted surface.

The optimum, or maximum, solar irradiation is received by an equator facing surface tilted at the optimal angle. The monthly climatology data represent the average of each month for the specified time period.

Another great data source is the Prediction Of Worldwide Energy Resources (POWER) project by NASA [45]. It was started with the primary goal of improving the present renewable energy data collection and creating new data sets using new satellite systems.

Photovoltaic Geographical Information System (PVGIS) offers free and open access to the following information:

PV potential for various technologies and configurations of grid-connected and stand-alone systems

Monthly averages or daily profiles of solar radiation and temperature

Hourly values of solar radiation and PV performance for the whole time series

Data for various climate variables from a typical meteorological year

Printable maps showing solar resource and PV potential by nation or area [46].

The tilt angle and azimuth angle are the two basic angles used to describe a PV array orientation, with the tilt angle being the vertical angle between the horizontal plane and the array surface. Fixing an appropriate tilt angle for a specific installation helps to capture the greatest irradiation intensity at a given surrounding situation. As a general rule, the tilt angle is set between the latitude of the location (φ) and (φ - 15°). The best tilt is determined by several factors such as mounting procedures, land topography, and environmental conditions [47].

The optimum tilt angle could be found using the NASA POWER source as well as the PVGIS. The optimum, or maximum, solar irradiation (kW-hr/m^2/day), which is received by an equator facing surface tilted at the optimal angle for each month is obtained from NASA POWER for the site location. This, along with the solar irradiation (kW-hr/m^2/day) at various tilt angles for a surface facing towards the equator and the optimal tilt is shown in Table 3-1. The data in each column are the average for over the month. According to the table, the optimal tilt is 13° throughout the year.

Global irradiation and solar electricity potential
Optimally-inclined photovoltaic modules

DJIBOUTI
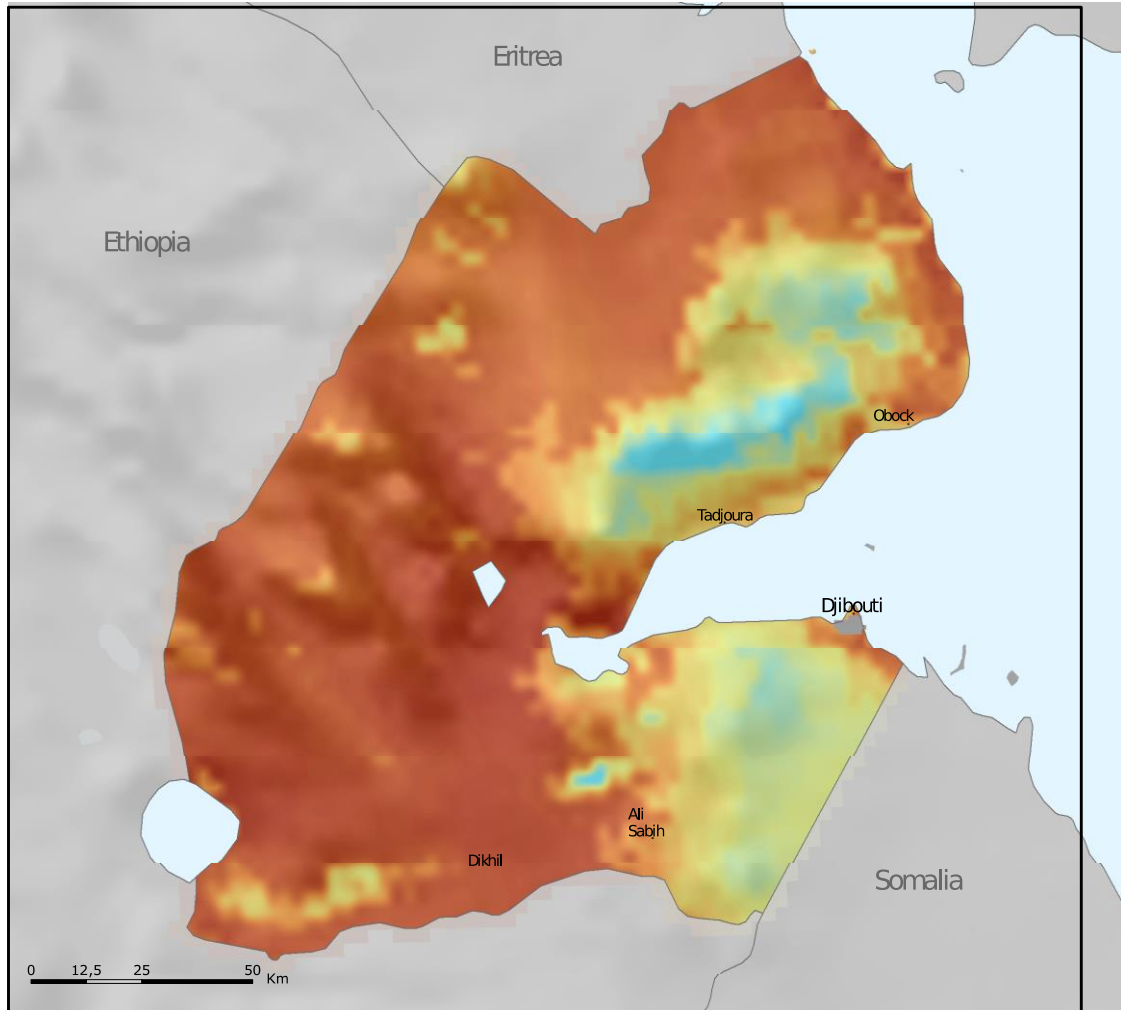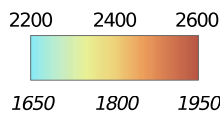
Figure 3.1 Global irradiation and solar electricity production potential in Djibouti [40].

Table 3-1 The solar irradiation at various tilt angles and the optimal tilt angles site-specific

Parameter	Jan	Feb	Mar	Apr	May	Jun	Jul	Aug	Sep	Oct	Nov	Dec
Solar irradiation horizontal surface (0°) (kW-hr/m^2/day)	5.06	5.65	6.21	6.56	6.58	6.15	5.78	6.05	6.35	6.11	5.55	5.15
Solar irradiation tilted surface at φ-15 (kW-hr/m^2/day)	5.2	5.76	6.27	6.54	6.51	6.07	5.72	6.02	6.37	6.2	5.71	5.32
Solar irradiation tilted surface at φ (kW-hr/m^2/day)	5.46	5.94	6.32	6.43	6.29	5.83	5.53	5.88	6.35	6.35	5.99	5.64
Solar irradiation tilted surface at φ+15 (kW-hr/m^2/day)	5.73	6.02	6.15	5.97	5.61	5.17	4.97	5.39	6.05	6.35	6.25	6
Solar irradiation vertical surface (90°) (kW-hr/m^2/day)	3.59	3.14	2.36	1.46	1.43	1.56	1.63	1.54	1.93	2.91	3.72	3.97
Solar irradiation tilted surface at optimal angle (kW-hr/m^2/day)	5.75	6.03	6.32	6.56	6.58	6.15	5.78	6.05	6.37	6.39	6.27	6.06
Optimal tilt (°)	32	23	11.5	0	0	0	0	0	5.5	19	30.5	35.5

The solar production time series data is obtained from the METEONORM database, version 8.0 trial. Reliable time series of solar irradiation with minute time precision is required to correctly simulate PV farms or energy management and storage systems. Lower resolution data is crucial while designing big PV plants or smaller plants containing energy storage, or involving self-consumption, and peak shaving. The difference between hourly and minute data is significant: with minute data, the fluctuation is greater, the ramps are steeper, and overshooting is more often.

Unfortunately, measuring minute values with ground sensors is difficult and expensive, and even impossible with satellite data. In order to keep up with industry demands, Meteonorm uses two methods to obtain minute resolution irradiation. The first method is the Hofmann model [48] included in the software. The other method is developed by Meteotest [49]. It is based on 15 real satellite minute measurements throughout the world adjusted for clear sky radiation and categorized by the cloud type, wind speed and solar elevation. Then using a stochastic generator, the minute time series is obtained based on the data.

The minute data is obtained using the Perez model [44] for a tilted surface of 13° and with the minute data using the Meteotest model. The results are shown in Table 3-2. The global irradiation for the tilted surface from METEONORM is 2302 kWh/m^2. The other sources results are as follows which confirm the accuracy of the data: the irradiation based on PVGIS is 2261 kWh/m^2 and renewable ninja [50] indicate 2310 kWh/m^2.

Table 3-2 The solar irradiation and other parameters for the site location from METEONORM software.

	Global horizontal radiation (kWh/m2)	Mean diffuse irradiance horizontal (kWh/m2)	Mean global irradiance, tilted plane (kWh/m2)	Irradiation of diffuse rad., tilted plane (kWh/m2)	Direct normal radiation (kWh/m2)	Air temperature (°C)	Wind speed (m/s)	Clear sky radiation (kWh/m2)	PV outpour (kWh/kWp)
Jan	182	45	208	50	216	23.9	6.6	193	156
Feb	171	59	186	64	164	24.4	6.5	180	139
Mar	202	70	209	73	181	26.3	6.2	221	153
Apr	220	61	216	62	214	28.3	5.7	223	156
May	204	83	193	81	163	30.8	4.3	219	139
Jun	177	92	166	89	108	32	5.3	197	119
Jul	179	93	169	90	109	32.8	6.2	205	121
Aug	177	97	172	96	99	32.7	5.4	207	123
Sep	180	81	182	82	132	31.5	4.2	207	131
Oct	193	68	205	72	174	28.9	5.1	205	149
Nov	178	49	200	54	196	26.2	6.3	190	148
Dec	171	49	197	55	195	24.9	6.4	183	147
Year	2234	845	2302	866	1953	28.5	5.7	2432	1683

* Latitude (°) = 11.54, Longitude (°) = 43.054, Altitude(m) = 103

3.2   Techno-economic data

The data used as an input to MicroGridPy are summarized in Table 3-3. The inputs are the techno-economical parameters of the project as well as PV, battery storage, and generators data. The discount rate of 10% is considered [51] for the economic assessment. The PV cost is very important in this analysis. According to IRENA, the cost of photovoltaics reduced by 85% from 2010 to 2020. The cost of producing electricity via PV is 0.8 $/W [52].

It should be mentioned that the cost of these systems is usually decreased by the size, and here a cost is chosen based on the approximate capacity of the microgrid. The battery energy system cost depends on the type of technology, self-discharge rate, round-trip efficiency, and lifetime. Here battery cost of 0.4 $/W is considered for the optimisation [53]. The life cycle of batteries is 5000 with an efficiency of charge and discharging of 96%.

The diesel generator is assumed to have an investment cost of 0.5 $/W and a lifecycle of 250000 hours of lifetime. This lifetime for the case of our optimisation is input as 13 years based on the working hours [54–56].

Table 3-3 The parameters of the techno-economical inputs.

Parameter	Value
General parameters	
Total duration of project (years)	20
Discount rate (%)	10
Photovoltaic Components	
Inverter efficiency	94
PV investment cost (k$/kW)	0.8
PV O&M cost (% as a fraction of specific investment cost)	3
PV lifetime (years)	20
Battery energy storage system	
Battery investment cost (k$/kWh)	0.4
Investment cost of balance of the system for batteries (k$/kWh)	0.2
Battery O&M cost (% as a fraction of specific investment cost)	2
Battery charge and discharge efficiency (%)	96
Battery depth of discharge (%)	80
Maximum charging and discharging time of batteries (h)	5
Battery lifetime (cycles)	5000
Generator parameters	
Generator efficiency (%)	33
Generator investment cost (k$/kW)	0.5
Generator O&M (% as a fraction of specific investment cost)	0.05
Generator lifetime (years)	13
Fuel cost ($/litre)	1
Fuel lower heat value (Wh/litre)	9840

3.3 Load demand

The load demand is another input for the optimization. due to computational limits, the load measured in Section 1.3.2 in minute resolution is reshaped into 15-minute resolution. The real power absorbed by the load is used for optimisation. It is assumed that the load is repeated as the measured week through the year.

Chapter 4
Results and discussion

4.1   Case studies and scenarios

To design the best microgrid system for the current load discussed in Section 1.3.2, several cases have been studied. The microgrid considered in this study consist of a PV array, battery bank, converter, diesel generator, and AC load.

Due to computational limitations, the 15-minute resolution load demand and PV production is used. Firstly, the optimisation of the given load is performed and considered as a base case for various scenarios to understand the feasibility of the system. The lost load, battery days of autonomy are set to 0. The renewable penetration is assumed unconstraint or equal to zero. The dispatch results for the first scenario are shown in Figure 4.1 and Figure 4.2 for three days in January and June, respectively.
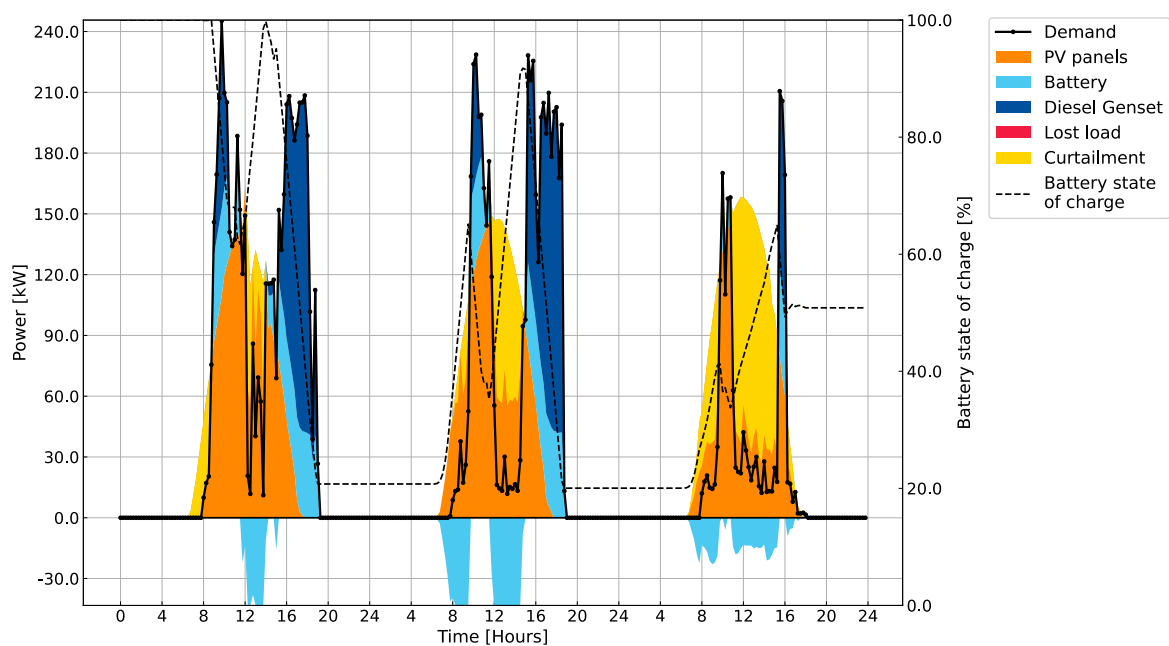
Figure 4.1 The dispatch plot of the optimal microgrid for three days in January
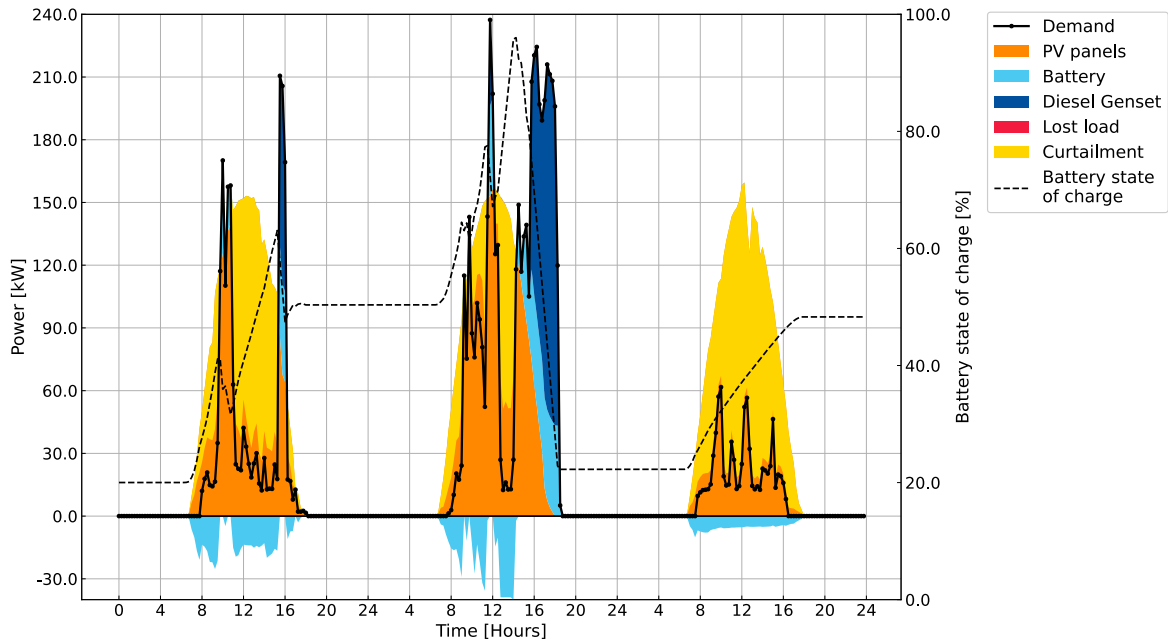
Figure 4.2 The dispatch plot of the optimal microgrid for three days in June.

The capacity of the studied microgrid components is shown in Table 4-1. Moreover, the economic result of the microgrid for 20 years of operation is summarized in Table 4-2. The Levelized Cost of Electricity (LCOE) is 0.255 USD/kWh, which is comparable with the grid cost of 0.253 USD/kWh in Djibouti. This is considered as a base case for the following comparisons and studies. The renewable energy penetration is 88%.

Table 4-1 The capacity of the optimal microgrid components.

Component	Unit	
PV panels	kW	308.13
Battery bank	kWh	868.49
Diesel Genset	kW	685.63

Table 4-2 The economic values of the base case microgrid.

Cost item	Component	Unit	Total
Net present cost	System	kUSD	2314.62
Total Investment cost	System	kUSD	1183.934
Total fixed O&M cost	System	kUSD	343.73
Total variable O&M cost	System	kUSD	786.966
Salvage value	System	kUSD	-0.011
Levelized Cost of Energy	System	USD/kWh	0.2548
	PV panels	kUSD	493.63
Investment cost	Battery bank	kUSD	347.443
	Diesel Genset	kUSD	342.862
	PV panels	kUSD	138.629
Fixed cost	Battery bank	kUSD	6.95
	Diesel Genset	kUSD	145.943
Lost load cost	System	kUSD	0
Replacement cost	Battery bank	kUSD	64.163
Fuel cost	Diesel	kUSD	722.803

4.1.1 Renewable energy penetration

To understand the effect of renewable energy penetration, the following study is conducted. The renewable energy penetration is fixed from 92 % to 100% and compared with the base case. Figure 4.3 The parameters of the optimal microgrid at various renewable penetrationsFigure 4.3 and Figure 4.4 show the results of this study. Increasing the renewable penetration leads to higher net present cost (NPC) and higher investment. In contrast, the operational cost is reduced. The investment increases by 232% when increasing the penetration from 88 to 100%. On the other hand, the operation cost is reduced by 40%. The energy curtailment is almost constant when the renewable penetration is in the range of 88-92% but increases to 53% at 100% penetration of renewable energy.

Renewable percentage	88.0%	92%	96%	100%
NPC k$	2314.62	2303.83	2384.55	2493.64
Total Investment Cost k$	1183.93	1400.01	1653.36	1966.67
Total Operation Cost k$	938.33	903.82	731.21	527.4
LCOE $/kWh	0.2357	0.2536	0.2625	0.295
Average battery usage %	13.88	20.34	27.25	27.23
Average curtailment %	45.43	45.94	44.49	53.06
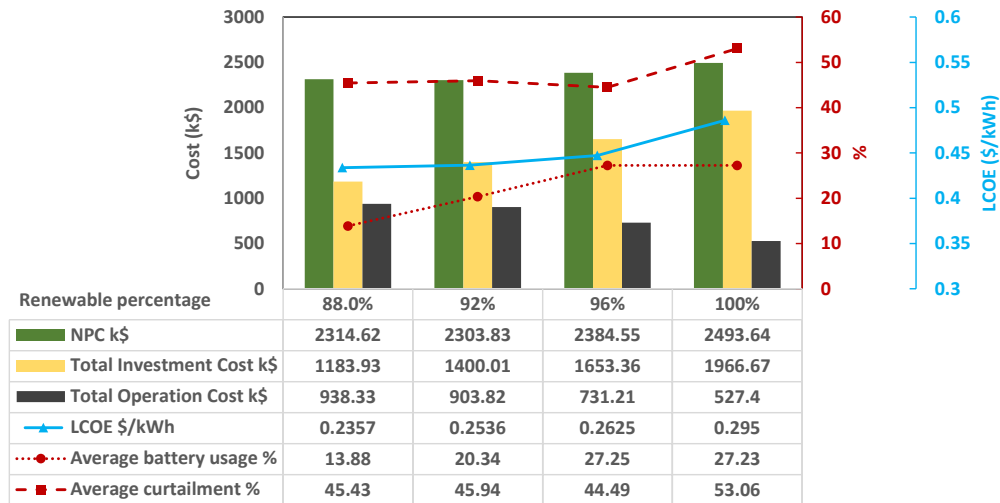
Figure 4.3 The parameters of the optimal microgrid at various renewable penetrations

According to Figure 4.4, the battery capacity should be as high as 4100 kWh when the renewable penetration is increased from 96% to 100%.

Renewable percentage	88.0%	92%	96%	100%
PV panels kW	308.13	320.57	328.65	389.52
Battery bank kWh	868.49	1432.8	2250.89	4109.71
Diesel Genset kW	685.63	546.41	379.58	0
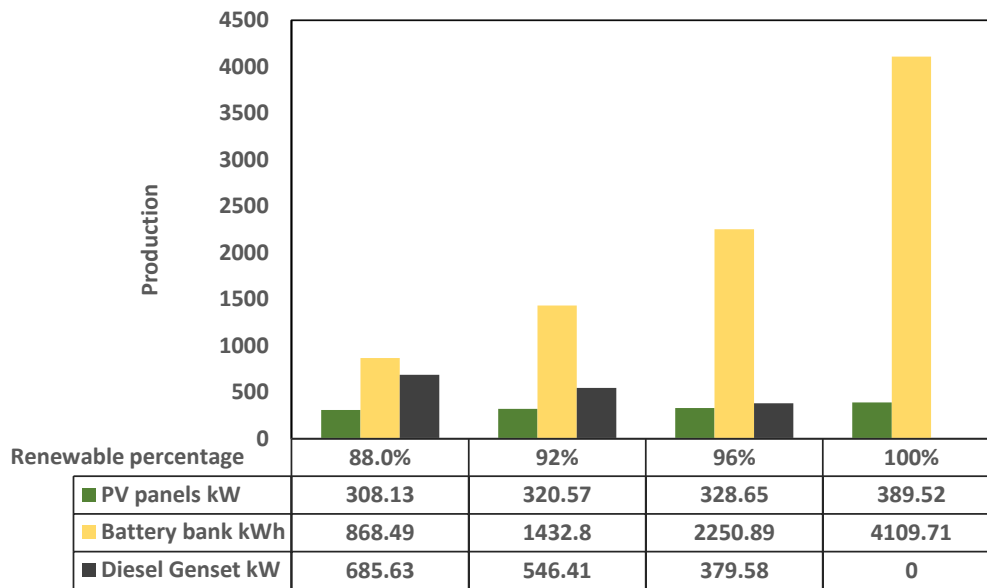
Figure 4.4 Energy parameters of the optimal microgrid at various renewable penetrations

4.1.2 Demand-side management

To minimize the curtailment and increase the share of renewable energy, demand-side management is required due to the intermittent solar power [57]. Here the daily load is shifted to match the solar production of the area so that the peak of solar production and load overlap. Studying the load shows that shifting the load by one hour and 15 minutes results in the best economic results. Figure 4.6 shows the dispatch results for the shifted optimised

case. As can be seen in the figure, the solar production hours meet the significant portion of demand with minimum curtailment.
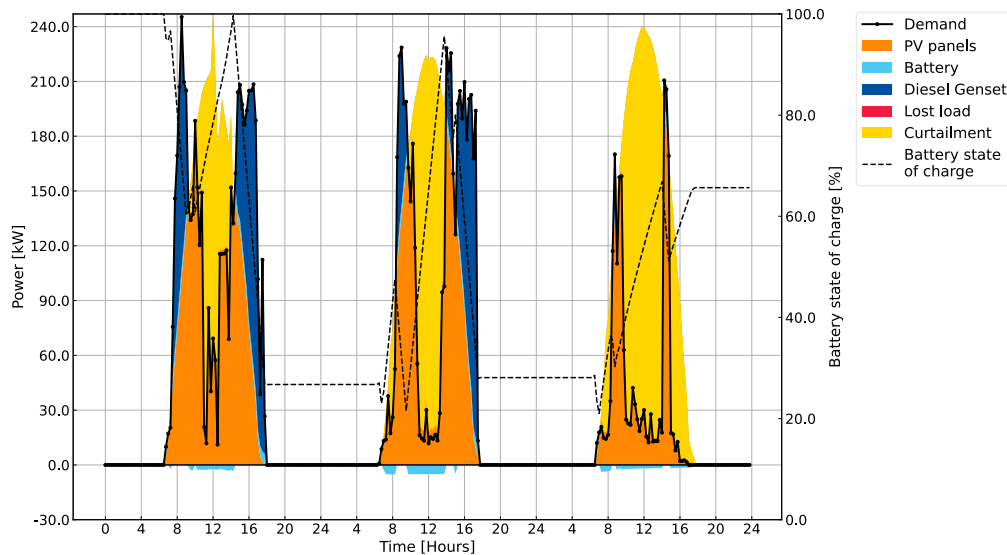
Figure 4.5 The dispatch plot of the optimal microgrid using demand-side management for three days in January.

The result of the optimisation is compared with the base case in Figure 4.6. The curtailment is reduced by 17.23%; the LCOE is reduced by 0.014 $/kWh. This shows the economic benefits of using demand-side management.

	Base case	Demand shift
NPC k$	2314.62	2015.08
Total Investment Cost k$	1183.93	1150.35
Total Operation Cost k$	938.33	864.73
LCOE $/kWh	0.2357	0.2218
Average battery usage %	13.88%	13.80%
Average curtailment %	45.43%	62.66%
Average renewable penetration per year %	88.00%	94.20%
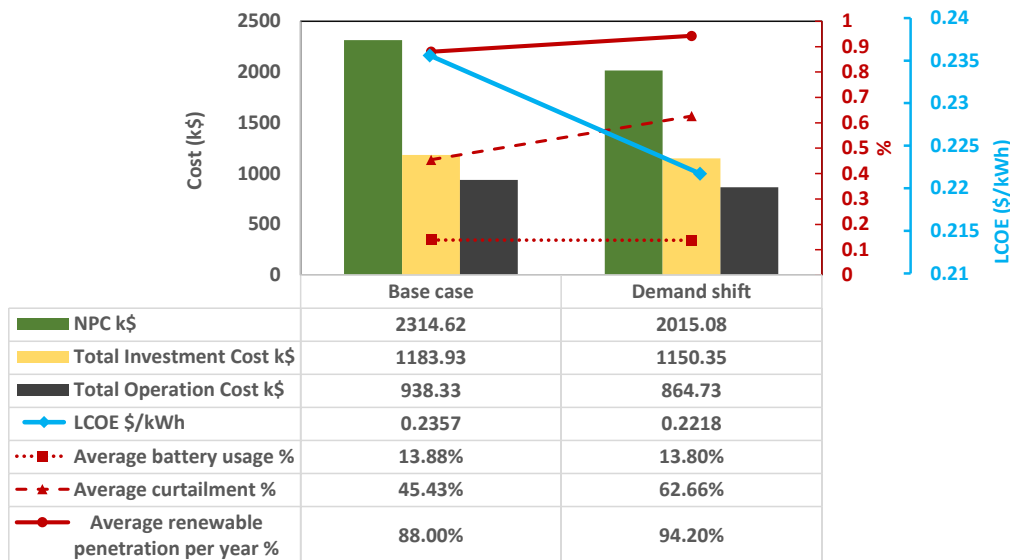
Figure 4.6 The results of the optimised microgrid using demand shift and the base case

4.1.3 Use of variable frequency drive

In this section, the feasibility of using a drive is studied. The variable frequency drive reduces the peak load demand while the system is starting. Therefore, the power is reduced accordingly. Here the power is assumed to remain below 175 kW as the case for using a drive, leading to 6.5% energy saving yearly. Figure 4.7 shows the dispatch result for this scenario.
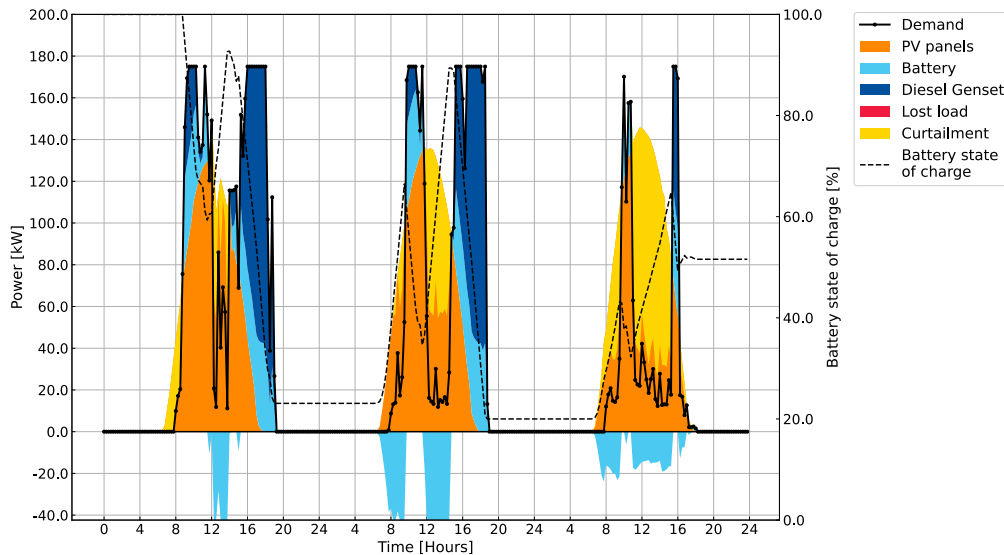
Figure 4.7 The dispatch plot of the optimal microgrid with a corrected load corresponding to the use of soft starters for three days in June

The optimisation results are shown in Figure 4.8. The results show that the net present and investment costs are reduced by 11% and 6%, respectively, while using a variable frequency drive. However, the battery usage and curtailed energy are constant. It should be noted that the operational cost should be further analysed since using a drive reduces the service and damages to the system.

	Base case	VFD
NPC k$	2314.62	2052.45
Total Investment Cost k$	1183.93	1114.12
Total Operation Cost k$	938.33	938.33
LCOE $/kWh	0.2357	0.242
Average battery usage %	13.88%	13.80%
Average curtailment %	45.43%	45.43%
Average renewable penetration per year %	88.00%	89.15%
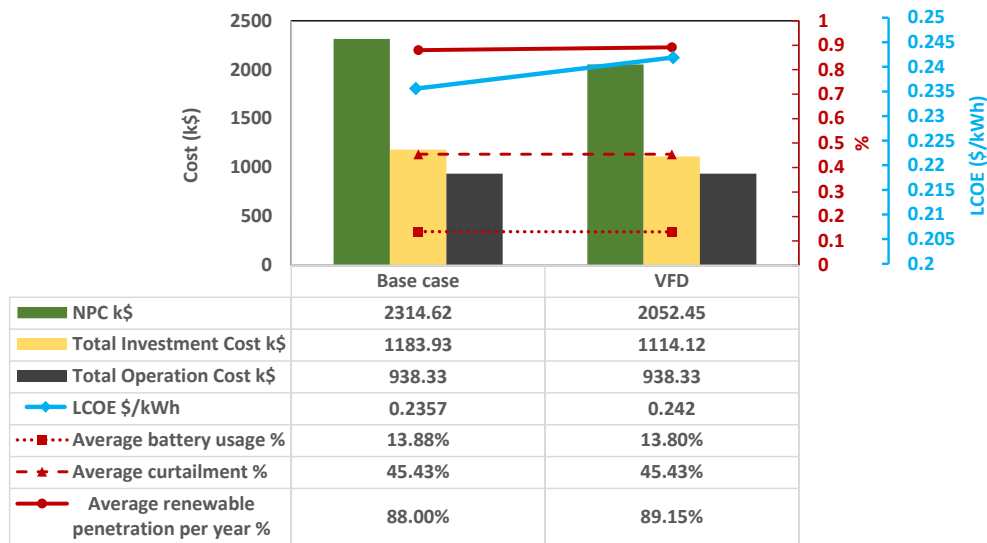
Figure 4.8 The results of the optimised system with a corrected load corresponding to the use VFD.

Figure 4.9 shows the system size obtained in this scenario. Compared to the base case the PV size, battery, and generator capacity are reduced by 8%, 2.5%, and 23%, respectively.

	Without VFD	With VFD
PV panels kW	308.13	283.58
Battery bank kWh	868.49	847.24
Diesel Genset kW	685.63	530.55

Figure 4.9 The system size of the optimised microgrid using soft starter and without VFD.

4.1.4   Two scenarios

To design a microgrid for future planning, a stochastic study is performed. Two scenarios are considered in the software MicroGridsPy. The first one is the present load, and the other scenario is the load with high consumption of 1,419 kWh per day.

Figure 4.10 shows the results of this analysis. According to the figure, the optimised microgrid would have 11% higher NPC, 13% higher investment cost, and 32% higher operational cost.

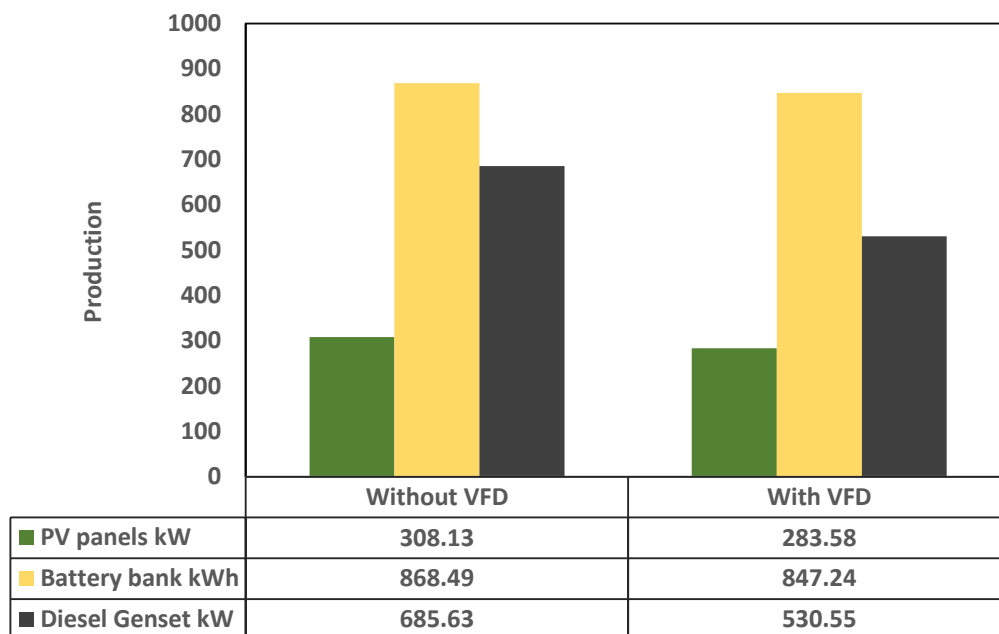|	Base case	2 scenarios
NPC k$	2314.62	2583.615
Total Investment Cost k$	1183.93	1342.473
Total Operation Cost k$	938.33	1241.16
LCOE $/kWh	0.2357	0.2539
Average battery usage %	13.88%	20.00%
Average curtailment %	45.43%	51.61%
Average renewable penetration per year %	88.00%	78.50%
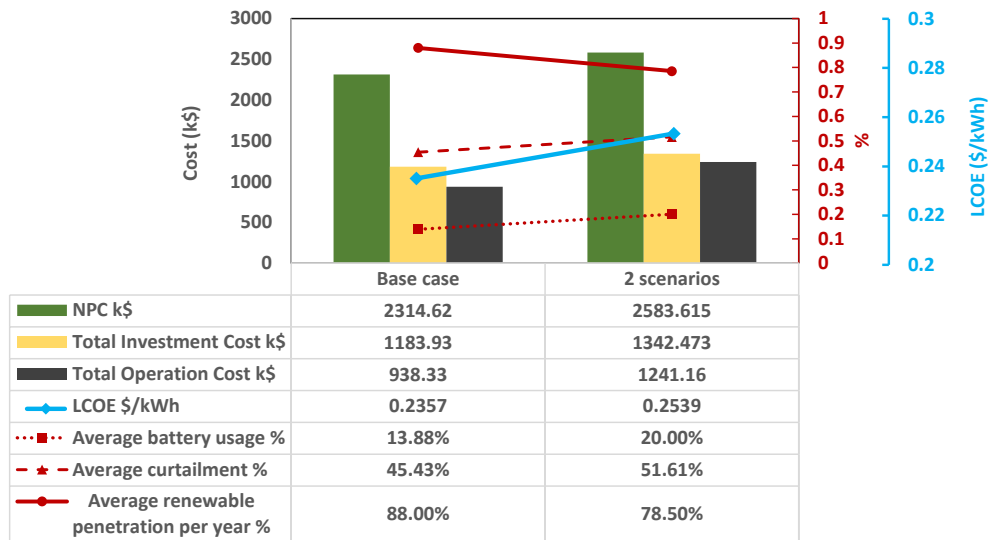
Figure 4.10 The results of the optimised system with 2 scenarios and the base case.

4.1.5   Sensitivity analysis

In this scenario, the maximum admittable lost load during the year is studied. The lost load is varied from 1% to 5%, Figure 4.11. As seen in Figure 4.12 the PV and battery bank capacities are reduced by 7% and 3% while increasing the lost load from 0% to 5%. The generator capacity is reduced significantly by 71% while reducing the lost load from 0 to 5%. The significant change in diesel generator capacity is due to the power peaks.
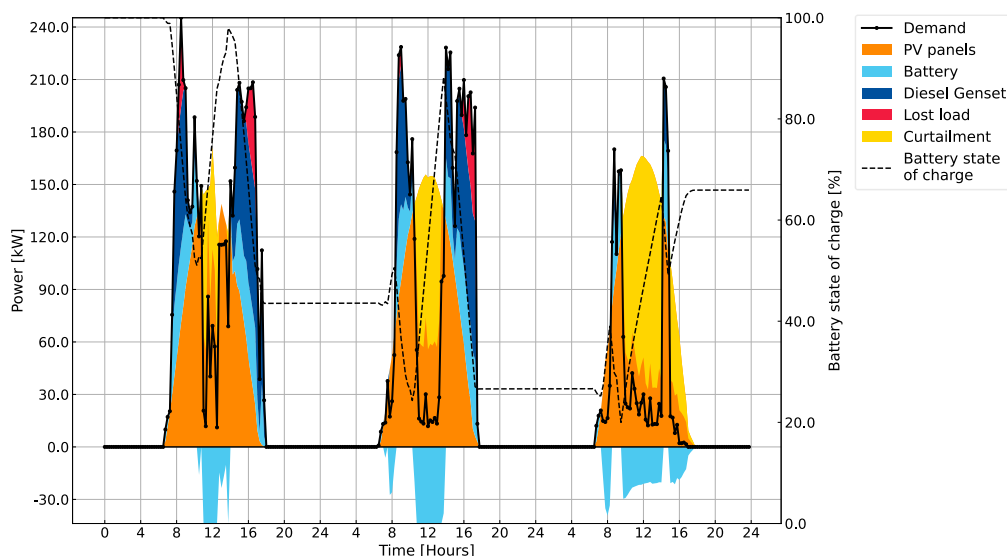
Figure 4.11 Dispatch result for three days in January allowable lost load is 1%.

Lost load percentage	0.0%	1.0%	2.0%	5%
▓ PV panels kW	308	325.32	323.52	331.13
■ Battery bank kWh	868.49	797.07	875.68	895.56
▩ Diesel Genset kW	685.63	397.05	317.11	195.15
■ Total Investment Cost kUSD	1183.93	1102.72	1090.12	1042.8
■ LCOE USD/MWh	235.7	235.6	226.8	206.9
■ Renewable penetration %	88	88.93	89.75	91.62

Figure 4.12 Lost load parameters comparison

Conclusions

The present study deals with the study and optimisation of microgrids, especially in industrial applications. The challenges and opportunities brought by decentralized power generation in the industry are discussed. A microgrid with highly variable loads in the Republic of Djibouti is investigated. First, the solutions for power instability issues are studied. Various sources are compared. Moreover, an optimisation using the open-source software MicroGridsPy based on mixed-integer linear programming (MILP) is performed to achieve an economi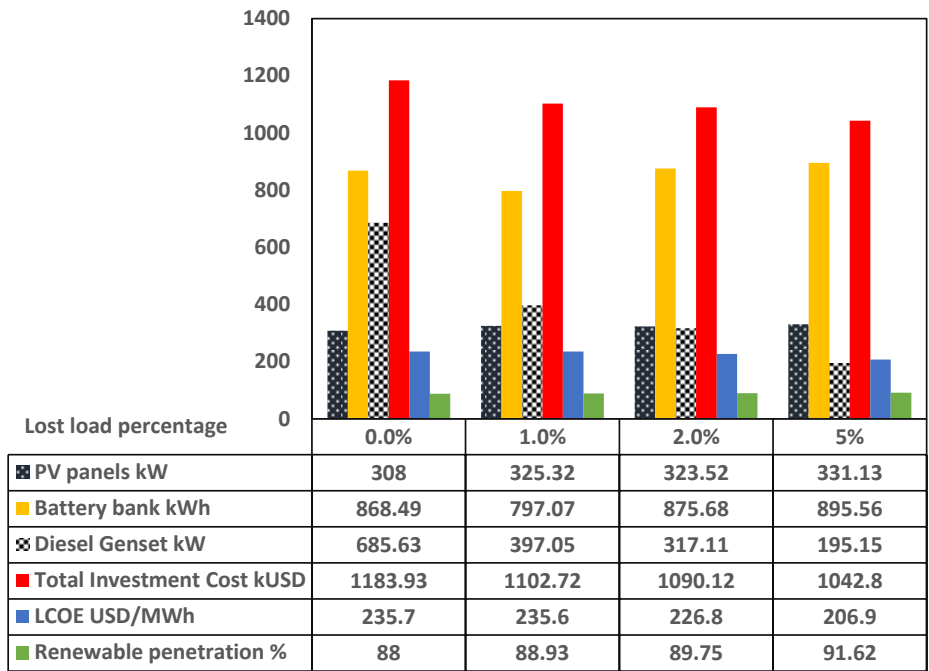cal hybrid microgrid design. Several scenarios are considered to analyse the working condition of the microgrid in various situations. The following are the key finding of this study:

- Two solutions of variable frequency drives and soft-starters are the most common economic practices for the starting power shock.

- According to the manufacturers, these power electronic devices have a short payback period of as low as two years.

- The most versatile sources for photovoltaic power generation are the Prediction Of Worldwide Energy Resources (POWER) project by NASA and METEONORM software, according to the literature and the results.

- Increasing the penetration from 88 to 100% led to a reduction of the operation cost by 40% and an increase of the investment cost by 200%.

- By shifting the demand to match the solar production, the curtailment is reduced by 17%, the LCOE is reduced by 0.014 $/kWh, and significant reductions occur in other economic parameters.

- In the scenario in which using the soft starters, the NPC and operational cost are reduced, while the LCOE, battery usage and curtailed energy are constant.

- The suggestions for future works are implementing the economy of scale while optimising since the costs of diesel generators, for example, reduce significantly with the size. Moreover, finding an optimising scheme in an industrial context, especially from a demand-side viewpoint, is an area for future study and development.

Acronyms

RES renewable energy sources

PV photovoltaic

Lat Latitude

Long Longitude

BESS battery energy storage system

DM demand-side management

DR Demand Response

MILP mixed-integer linear programming

YC yearly cost

EB Energy stored in batteries

LL lost load

DOD depth of discharge

SOC state of charge

Bibliography

[1]   Chandak S, Rout PK. The implementation framework of a microgrid: A review. International Journal of Energy Research 2021;45:3523–47. https://doi.org/10.1002/ER.6064.

[2]   IEC 60050 - International Electrotechnical Vocabulary - Details for IEV number 617-04-22: "microgrid" n.d. https://www.electropedia.org/iev/iev.nsf/display?openform&ievref=617-04-22 (accessed October 25, 2021).

[3]   Wang J, Costa LM, Cisse BM. From distribution feeder to microgrid: An insight on opportunities and challenges. 2016 IEEE International Conference on Power System Technology, POWERCON 2016 2016. https://doi.org/10.1109/POWERCON.2016.7753897.

[4]   Kzaviri SM, Pahlevani M, Jain P, Bakhshai A. A review of AC microgrid control methods. 2017 IEEE 8th International Symposium on Power Electronics for Distributed Generation Systems, PEDG 2017 2017. https://doi.org/10.1109/PEDG.2017.7972498.

[5]   Bernardi E, Morato MM, Mendes PRC, Normey-Rico JE, Adam EJ. Fault-tolerant energy management for an industrial microgrid: A compact optimization method. International Journal of Electrical Power & Energy Systems 2021;124:106342. https://doi.org/10.1016/J.IJEPES.2020.106342.

[6]   IEC 60050 - International Electrotechnical Vocabulary - Details for IEV number 617-04-23: "isolated microgrid" n.d. https://www.electropedia.org/iev/iev.nsf/display?openform&ievref=617-04-23 (accessed October 25, 2021).

[7]   Guarnieri M, Bovo A, Giovannelli A, Mattavelli P. A Real Multitechnology Microgrid in Venice: A Design Review. IEEE Industrial Electronics Magazine 2018;12:19–31. https://doi.org/10.1109/MIE.2018.2855735.

[8]   ALAIMO A, ZANOLINI AM. DESIGN OF A MODEL FOR MICRO-GRID SIMULATIONS: THE CASE OF ST. MARY'S LACOR HOSPITAL. 2017.

[9]   IEA (2021), World Energy Balances: Overview, IEA, Paris https://www.iea.org/reports/world-energy-balances-overview. n.d.

[10]   Blake ST, O'Sullivan DTJ. Optimization of Distributed Energy Resources in an Industrial Microgrid. Procedia CIRP 2018;67:104–9. https://doi.org/10.1016/J.PROCIR.2017.12.184.

[11]   Choobineh M, Mohagheghi S. A multi-objective optimization framework for energy and asset management in an industrial Microgrid. Journal of Cleaner Production 2016;139:1326–38. https://doi.org/10.1016/J.JCLEPRO.2016.08.138.

[12]   Leif Hanrahan B, Lightbody G, Staudt L, Leahy PG. A powerful visualization technique for electricity supply and demand at industrial sites with combined heat and power and wind generation. Renewable and Sustainable Energy Reviews 2014;31:860–9. https://doi.org/10.1016/J.RSER.2013.12.016.

[13]   Zheng Y, Jenkins BM, Kornbluth K, Kendall A, Træholt C. Optimization of a biomass-integrated renewable energy microgrid with demand side management under uncertainty. Applied Energy 2018;230:836–44. https://doi.org/10.1016/J.APENERGY.2018.09.015.

[14]   Logenthiran T, Srinivasan D, Shun TZ. Demand side management in smart grid using heuristic optimization. IEEE Transactions on Smart Grid 2012;3:1244–52. https://doi.org/10.1109/TSG.2012.2195686.

[15]   Logenthiran T, Srinivasan D, Shun TZ. Demand side management in smart grid using heuristic optimization. IEEE Transactions on Smart Grid 2012;3:1244–52. https://doi.org/10.1109/TSG.2012.2195686.

[16]   Gamarra C, Guerrero JM, Montero E. A knowledge discovery in databases approach for industrial microgrid planning. Renewable and Sustainable Energy Reviews 2016;60:615–30. https://doi.org/10.1016/J.RSER.2016.01.091.

[17]   Lu R, Bai R, Ding Y, Wei M, Jiang J, Sun M, et al. A hybrid deep learning-based online energy management scheme for industrial microgrid. Applied Energy 2021;304:117857. https://doi.org/10.1016/J.APENERGY.2021.117857.

[18]   Zhang R, Li G, Jiang T, Chen H, Li X, Pei W, et al. Incorporating Production Task Scheduling in Energy Management of an Industrial Microgrid: A Regret-Based Stochastic Programming Approach. IEEE Transactions on Power Systems 2021;36:2663–73. https://doi.org/10.1109/TPWRS.2020.3037831.

[19]   Eseye AT, Zhang J, Zheng D, Wei D. Optimal energy management strategy for an isolated industrial microgrid using a modified particle swarm optimization. 2016 IEEE International Conference on Power and Renewable Energy, ICPRE 2016 2017:494–8. https://doi.org/10.1109/ICPRE.2016.7871126.

[20]   Naderi M, Bahramara S, Khayat Y, Bevrani H. Optimal planning in a developing industrial microgrid with sensitive loads. Energy Reports 2017;3:124–34. https://doi.org/10.1016/J.EGYR.2017.08.004.

[21]   Supercapacitor - Wikipedia n.d. https://en.wikipedia.org/wiki/Supercapacitor#Energy_capacity (accessed December 5, 2021).

[22]   Motor soft starter - Wikipedia n.d. https://en.wikipedia.org/wiki/Motor_soft_starter (accessed October 27, 2021).

[23]   Kjellberg M, Sören Kling. Softstarter handbook. ABB Automation Technology Product AB; 2003.

[24]   Lönnberg M. Variable Speed Drives for energy savings in hospitals. World Pumps 2007;2007:20–4. https://doi.org/10.1016/S0262-1762(07)70395-4.

[25]   Drives ABB. Technical guide No. 4 Guide to variable speed drives. Specifications Subject to Change without Notice 3AFE61389211 REVC12, 5 2011.

[26]   Products - Delixi inverter n.d. http://www.delixidrive.com/list-112-1.html (accessed October 30, 2021).

[27]   Djibouti | Data n.d. https://data.worldbank.org/country/DJ (accessed November 4, 2021).

[28]   Djibouti | History, Capital, Map, Flag, Population, & Facts | Britannica n.d. https://www.britannica.com/place/Djibouti (accessed November 24, 2021).

[29]   Hegedus S, and AL-H of photovoltaic science, 2003 undefined. Status, trends, challenges and the bright future of solar electricity from photovoltaics. Citeseer n.d.

[30]   Dufo-López R, Cristóbal-Monreal IR, Yusta JM. Optimisation of PV-wind-diesel-battery stand-alone systems to minimise cost and maximise human development index and job creation.   Renewable   Energy   2016;94:280–93. https://doi.org/10.1016/J.RENENE.2016.03.065.

[31]   Zubi G, Dufo-López R, Pasaoglu G, Pardo N. Techno-economic assessment of an off-grid PV system for developing regions to provide electricity for basic domestic needs: A 2020– 2040   scenario.   Applied   Energy   2016;176:309–19. https://doi.org/10.1016/J.APENERGY.2016.05.022.

[32]   Vision 2035 – Policies - IEA n.d. https://www.iea.org/policies/6011-vision-2035 (accessed November 4, 2021).

[33]   Myrsalieva N, Åberg E, Mahmoud M. Arab Future Energy Index™(AFEX) Renewable Energy 2015. Cairo, Egypt: Regional Center for Renewable Energy and Energy Efficiency (RCREEE) 2015 n.d.

[34]   IRENA, IREA. Renewable power generation costs in 2017. International Renewable Energy Agency, Abu Dhabi (2018) n.d.

[35]   Balderrama S, Haderspock F, … WC-… 2018-P of, 2018 undefined. Techno-economic evaluation of rural electrification in Bolivia: lessons learned from the "El Espino" micro-grid. LiriasKuleuvenBe n.d.

[36]   Stevanato N, Lombardi F, Guidicini G, Rinaldi L, Balderrama SL, Pavičević M, et al. Long-term sizing of rural microgrids: Accounting for load evolution through multi-step investment plan and stochastic optimization. Energy for Sustainable Development 2020;58:16–29. https://doi.org/10.1016/J.ESD.2020.07.002.

[37]   Stevanato N, Lombardi F, Guidicini G, Rinaldi L, Balderrama SL, Pavičević M, et al. Long-term sizing of rural microgrids: Accounting for load evolution through multi-step investment plan and stochastic optimization. Energy for Sustainable Development 2020;58:16–29. https://doi.org/10.1016/J.ESD.2020.07.002.

[38]   Balderrama S, Lombardi F, Riva F, Energy WC-, 2019 undefined. A two-stage linear programming optimization framework for isolated hybrid microgrids in a rural context: The case study of the "El Espino" community. Elsevier n.d.

[39]   Stevanato N, Lombardi F, Colmbo E, Balderrama S, Quoilin S. Two-stage stochastic sizing of a rural micro-grid based on stochastic load generation. 2019 IEEE Milan PowerTech, PowerTech 2019 2019. https://doi.org/10.1109/PTC.2019.8810571.

[40]   Pillot B, Muselli M, Poggi P, Dias JB. Satellite-based assessment and in situ validation of solar irradiation maps in the Republic of Djibouti. Solar Energy 2015;120:603–19. https://doi.org/10.1016/J.SOLENER.2015.08.015.

[41] Gueymard CA, Myers DR. Validation and Ranking Methodologies for Solar Radiation Models. Modeling Solar Radiation at the Earth's Surface: Recent Advances 2008:479–510. https://doi.org/10.1007/978-3-540-77455-6_20.

[42] da Silva MK, Narvaez DI, de Melo KB, Villalva MG. Comparative analysis of transposition models applied to photovoltaic systems using meteonorm and NASA SSE databases. 2018 13th IEEE International Conference on Industry Applications, INDUSCON 2018 - Proceedings 2019:237–41. https://doi.org/10.1109/INDUSCON.2018.8627354.

[43] da Silva MK, Narvaez DI, de Melo KB, Villalva MG. Comparative analysis of transposition models applied to photovoltaic systems using meteonorm and NASA SSE databases. 2018 13th IEEE International Conference on Industry Applications, INDUSCON 2018 - Proceedings 2019:237–41. https://doi.org/10.1109/INDUSCON.2018.8627354.

[44] Perez R, Ineichen P, Seals R, Michalsky J, Stewart R. Modeling daylight availability and irradiance components from direct and global irradiance. Solar Energy 1990;44:271–89. https://doi.org/10.1016/0038-092X(90)90055-H.

[45] NASA POWER | Prediction Of Worldwide Energy Resources n.d. https://power.larc.nasa.gov/#resources (accessed November 1, 2021).

[46] Photovoltaic Geographical Information System (PVGIS) | EU Science Hub n.d. https://ec.europa.eu/jrc/en/pvgis (accessed November 1, 2021).

[47] Mamun MAA, Islam MM, Hasanuzzaman M, Selvaraj J. Effect of tilt angle on the performance and electrical parameters of a PV module: Comparative indoor and outdoor experimental investigation. Energy and Built Environment 2021. https://doi.org/10.1016/J.ENBENV.2021.02.001.

[48] Hofmann M, Riechelmann S, Crisosto C, Mubarak R, Seckmeyer G. Improved synthesis of global irradiance with one-minute resolution for PV system simulations. International Journal of Photoenergy 2014;2014. https://doi.org/10.1155/2014/808509.

[49] Remund J. Generation of one minute data 2016.

[50] Renewables.ninja n.d. https://www.renewables.ninja/ (accessed November 2, 2021).

[51] plan LE-D national biodiversity strategy and action, 1998 undefined. Djibouti biodiversity: economic assessment. ResearchgateNet 1998.

[52] IRENA (2021), Renewable Power Generation Costs in 2020, International Renewable Energy Agency, Abu Dhabi. n.d.

[53] IRENA (2017), Electricity Storage and Renewables: Costs and Markets to 2030, International Renewable Energy Agency, Abu Dhabi. n.d.

[54] Bukar AL, Tan CW, Lau KY. Optimal sizing of an autonomous photovoltaic/wind/battery/diesel generator microgrid using grasshopper optimization algorithm. Solar Energy 2019;188:685–96. https://doi.org/10.1016/J.SOLENER.2019.06.050.

[55] Adefarati T, Bansal RC, Justo JJ. Reliability and economic evaluation of a microgrid power system. Energy Procedia 2017;142:43–8. https://doi.org/10.1016/J.EGYPRO.2017.12.008.

[56]   Bhattacharyya SC. Mini-grid based electrification in Bangladesh: Technical configuration and business analysis. Renewable Energy 2015;75:745–61. https://doi.org/10.1016/J.RENENE.2014.10.034.

[57]   Finn P, Fitzpatrick C. Demand side management of industrial electricity consumption: Promoting the use of renewable energy through real-time pricing. Applied Energy 2014;113:11–21. https://doi.org/10.1016/J.APENERGY.2013.07.003.